AD-A151 414 EFFECTS OF FINITE CURRENT CHANNEL WIDTH ON THE CURRENT CONVECTIVE INSTABILITY(U) NAVAL RESEARCH LAB WASHINGTON DC P SATYANARAYANA ET AL. 05 MAR 85 NRL-MR-5494 1/1

UNCLASSIFIED F/G 20/9 NL

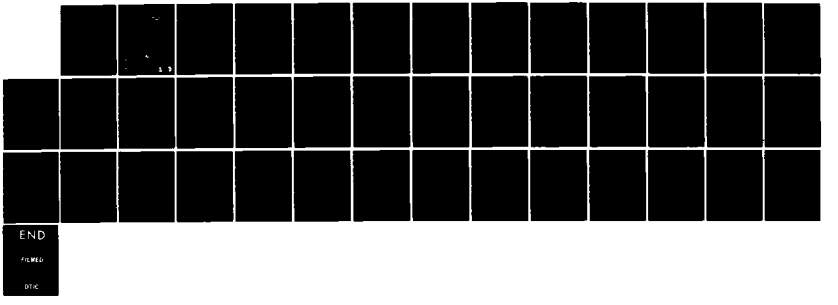

END

FILMED

DTIC

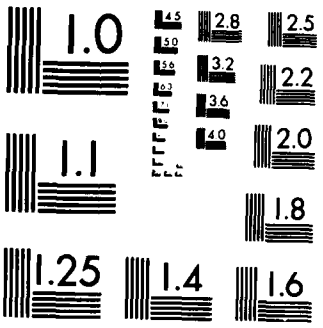

NRL Memorandum Report 5404

Effects of Finite Current Channel Width on the Current Convective Instability

P. SATYANARAYANA AND J. CHEN

Science Applications, Inc.
McLean, VA 22102

M. J. KESKINEN

Geophysical and Plasma Dynamics Branch
Plasma Physics Division

March 5, 1985

This research was partially sponsored by the Office of Naval Research and the Defense Nuclear Agency under Subtask S99QMXBC, work unit 00102 and work unit title "Plasma Structure Evolution."

NAVAL RESEARCH LABORATORY
Washington, D.C.

SECURITY CLASSIFICATION OF THIS PAGE

REPORT DOCUMENTATION PAGE

1a REPORT SECURITY CLASSIFICATION UNCLASSIFIED	1b RESTRICTIVE MARKINGS
2a SECURITY CLASSIFICATION AUTHORITY	3 DISTRIBUTION / AVAILABILITY OF REPORT Approved for public release; distribution unlimited.
2b DECLASSIFICATION / DOWNGRADING SCHEDULE	
4 PERFORMING ORGANIZATION REPORT NUMBER(S) NRL Memorandum Report 5494	5 MONITORING ORGANIZATION REPORT NUMBER(S)
6a NAME OF PERFORMING ORGANIZATION Naval Research Laboratory 6b OFFICE SYMBOL (If applicable) Code 4780	7a NAME OF MONITORING ORGANIZATION
6c ADDRESS (City, State, and ZIP Code) Washington, DC 20375-5000	7b ADDRESS (City, State, and ZIP Code)
8a NAME OF FUNDING / SPONSORING ORGANIZATION ONR and DNA 8b OFFICE SYMBOL (If applicable)	9 PROCUREMENT INSTRUMENT IDENTIFICATION NUMBER
8c ADDRESS (City, State, and ZIP Code) Arlington, VA 22217 Washington, DC 20305	10 SOURCE OF FUNDING NUMBERS PROGRAM ELEMENT NO (See page ii) / PROJECT NO / TASK NO / WORK UNIT ACCESSION NO

11 TITLE (Include Security Classification)

Effects of Finite Current Channel Width on the Current Convective Instability

12 PERSONAL AUTHOR(S)
Satyanarayana, P.,* Chen, J.* and Keskinen, M.J.

13a TYPE OF REPORT	13b TIME COVERED	14 DATE OF REPORT (Year, Month, Day)	15 PAGE COUNT
Interim	FROM 10/83 TO 10/84	1985 March 5	41

16 SUPPLEMENTARY NOTATION

*Science Applications, Inc., McLean, VA 22102 (Continues)

17 COSATI CODES			18 SUBJECT TERMS (Continue on reverse if necessary and identify by block number)
FIELD	GROUP	SUB-GROUP	Plasma instability; Fluid instability; High latitude ionosphere; Finite current channel width

19 ABSTRACT (Continue on reverse if necessary and identify by block number)

The effects of the finite current channel width on the current convective instability are studied both analytically and numerically. First using a sharp-boundary field-aligned current distribution which has a finite width along the plasma density gradient, the dispersion relation is obtained analytically. It is found that, for the long wavelength modes ($k_y d \ll 1$) where the nonlocal effects are most prominent, the growth rate γ is proportional to $|\overline{V}_d d/L^2|$ in the collisional limit ($\nu_{in} \gg |\omega|$), (Continues)

20 DISTRIBUTION / AVAILABILITY OF ABSTRACT	21 ABSTRACT SECURITY CLASSIFICATION
☒ UNCLASSIFIED/UNLIMITED ☐ SAME AS RPT ☐ DTIC USERS	UNCLASSIFIED
22a NAME OF RESPONSIBLE INDIVIDUAL J. D. Huba	22b TELEPHONE (Include Area Code) (202) 767-3630 / 22c OFFICE SYMBOL Code 4780

DD FORM 1473, 84 MAR 83 APR edition may be used until exhausted
All other editions are obsolete

SECURITY CLASSIFICATION OF THIS PAGE

10. SOURCE OF FUNDING NUMBERS

PROGRAM ELEMENT NO.	PROJECT NO.	TASK NO.	WORK UNIT ACCESSION NO.
62715H 61153N		RR033-02-44	DN880-024 DN230-291

16. SUPPLEMENTARY NOTATION (Continued)

This research was partially sponsored by the Office of Naval Research and the Defense Nuclear Agency under Subtask S99QMXBC, work unit 00102 and work unit title "Plasma Structure Evolution."

19. ABSTRACT (Continued)

where d is the half-width of the current channel, L is the plasma density gradient scale length, $\overline{V}_d$ is the field-aligned current velocity, ν_{in} is the ion-neutral collision frequency and ω is the perturbation frequency. For the long wavelength modes in the inertial limit ($\nu_{in} \ll |\omega|$), the growth rate γ scales as $|\overline{V}_d d/L^2|^{\alpha}$, where $\alpha = 1/2$ (2/3) for $k_z^2/k_y^2\, \Omega_e/\nu_{ei}$ much less than (greater than) $|\omega|/\Omega_i$ and $k_z(k_y)$ is the wavenumber parallel (perpendicular) to the magnetic field, $\Omega_e(\Omega_i)$ is the electron (ion) gyrofrequency, and ν_{ei} is the electron-ion collision frequency. Numerical results are also presented for a diffuse-boundary current velocity distribution. Applications to the high latitude ionosphere are discussed.

CONTENTS

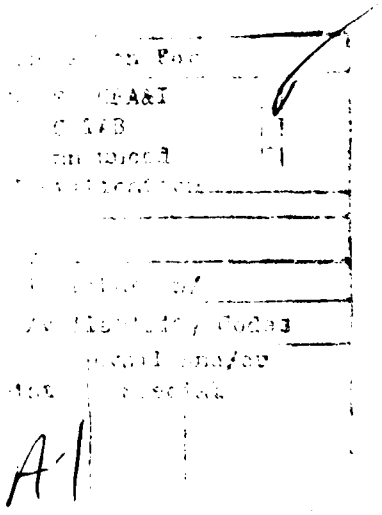

EFFECTS OF FINITE CURRENT CHANNEL WIDTH ON THE CURRENT CONVECTIVE INSTABILITY

I. INTRODUCTION

From a variety of experimental observations [see recent reviews by Fejer and Kelley, 1980, Vickrey and Kelley, 1983, and Hanuise et al., 1981], it is now known that the high latitude ionosphere, from the auroral zone into the polar cap, is a highly structured and nonequilibrium medium containing plasma fluctuations and structures with scale sizes ranging from hundreds of kilometers to meters. Several processes, e.g., particle precipitation, plasma instabilities, and neutral fluid dynamics, have been proposed to account for high latitude ionospheric plasma structure [Keskinen and Ossakow, 1983a]. The plasma instabilities that have received the most attention thus far are the ExB instability [Simon, 1963; Linson and Workman, 1970; Keskinen and Ossakow, 1982, 1983b; Huba et al; 1983, Keskinen, 1984] and the current convective instability [Lehnert, 1958; Kadomtsev and Nedospasov, 1960; Ossakow and Chaturvedi, 1979; Huba and Ossakow, 1980; Keskinen et al., 1980; Chaturvedi and Ossakow, 1981, 1983; Satyanarayana and Ossakow, 1984; Gary, 1984; Huba, 1984]. The current convective instability results from the coupling of a magnetic field-aligned current and a plasma density gradient transverse to the magnetic field in the presence of electron-neutral collisions -- a configuration likely to occur in the auroral zone ionosphere [Vickrey et al., 1980]. All of the previous studies of the current convective instability have assumed that the width of the current transverse to the magnetic field is infinite. However, recent observational results [see, for example, Bythrow et al., (1984)] indicate that the transverse dimension of the field-aligned current distributions may be comparable to or less than the density gradient scale length. Since the instability requires both a density gradient and a field-aligned current, the properties of the instability may be modified if one uses a more realistic geometry with a current channel of finite width. Indeed, physical intuition would lead one to expect reduction in the growth rate and modification in the stability boundary for narrow current channels. In this analysis we remove the infinite-width current simplification and study the effects of finite current channel width on the current convective instabiity. The analytical and numerical

Manuscript approved October 4, 1984.

results will show that, in the long wavelength limit, $k_y d \ll 1$, where the nonlocal results are most prominent, the growth rate depends on the global quantities such as $(\bar{V}_d d/L^2)$, where $\bar{V}_d$ is the current velocity, d is the half-width of the current channel and L is the density gradient scale length. These intrinsically nonlocal effects may be of interest for interpretation of the observational data. We discuss the nonlocal results and apply them to the high latitude ionosphere.

The organization of the paper is as follows. In Section II we derive the general dispersion relation describing the mode structure of the current convective instability with a finite current channel width. In Section III we present a theoretical analysis of the mode structure equation while in Section IV we give numerical results. Finally, in Section V we summarize our findings and discuss applications to the high latitude ionosphere.

II. MODE STRUCTURE EQUATION

In this paper we use a slab model shown in Fig. (1). The plasma is assumed inhomogeneous along the north-south direction ($\hat{x}$) and is assumed to support equilibrium currents along the magnetic field. The magnetic field is uniform and vertical ($\hat{z}$) with the field-aligned currents taken to be of the form $\underline{J} = J_o(x)\,\hat{z}$. The primary objective of this paper is to confine the field-aligned currents to a finite region along the direction of the density gradient ($\hat{x}$) and to study the effects of finite current width on the current convective instability. We neglect weak altitude dependent density gradients as well as east-west ($\hat{y}$) gradients and transverse equilibrium electric fields. The temperature effects responsible for diffusive damping are ignored as is magnetic field shear. Electron inertia is neglected since current convective instability is a low frequency instability ($\omega \ll \Omega_e$). Furthermore, we confine ourselves to the F-region of the ionosphere and ignore the electron-neutral collision frequency (ν_{en}) compared to the electron-ion collision frequency (ν_{ei}). Due to the variation of the field-aligned currents and the background density along x, we perform a nonlocal analysis and derive a mode structure equation for the perturbed potential. This procedure allows us to study short wavelength and long wavelength modes. The basic two-fluid equations

describing the electron and ion dynamics in the rest frame of the neutrals are

$$\frac{\partial n_\alpha}{\partial t} + \nabla \cdot (n_\alpha \underline{V}_\alpha) = 0 , \tag{1}$$

$$m_\alpha n_\alpha \left(\frac{\partial}{\partial t} + \underline{V}_\alpha \cdot \nabla\right) \underline{V}_\alpha = q_\alpha n_\alpha \left(\underline{E} + \frac{\underline{V}_\alpha \times \underline{B}}{c}\right) - m_\alpha n_\alpha \nu_{\alpha n} \underline{V}_\alpha - \underline{R}_\alpha , \tag{2}$$

where α denotes species (e for electrons; i for ions), n_α is the plasma density, $\underline{V}$ is the fluid velocity, m_α is the mass of the species, q_α is the charge of the species, c is the speed of light, $\underline{E}$ is the electric field, $\nu_{\alpha n}$ is the plasma particle collision frequency with neutrals, and $\underline{R}_\alpha$ is the friction force given by

$$R_i = m_i n_i \nu_{ie} (\underline{V}_i - \underline{V}_e) , \tag{3}$$

$$R_e = m_e n_e \nu_{ei} (\underline{V}_e - V_i). \tag{4}$$

The equilibrium velocities are given by

$$V_{ez}^0 = - \frac{e E_{0z}}{m_e \nu_{ei}} \tag{5}$$

$$V_{iz}^0 = 0 \tag{6}$$

In obtaining these equations, terms proportional to $\nu_{en}/\Omega_e << 1$ have been neglected. By setting $\underline{E}_{0\perp} = 0$, it can be easily shown that $\underline{V}_{e\perp} = \underline{V}_{i\perp} = 0$. We choose the friction force to be $R_e = - R_i$ so that momentum conservation demands $\nu_{ie} m_i = \nu_{ei} m_e$ and thus $V_{iz}^0 = 0$. The net drift velocity $V_d \equiv V_{ez}^0 - V_{iz}^0$ then becomes $V_d = V_{ez}^0$. More generally, however, neutral particles also participate in momentum conservation, and V_{iz}^0 need not be zero. The above simplification implies that the electrons are the primary current carriers.

In order to derive the nonlocal mode structure equation, we use a perturbation of the form $\hat{f} \sim f(x) \exp[-i(\omega t - k_y y - k_z z)]$, where $\omega = \omega_r + i\gamma$, $\gamma > 0$ for growth and k_y and k_z are the mode numbers in y and z directions. We then linearize Eqs. (1) and (2), and finally we subtract the electron continuity equation from the ion continuity equation [Eq. (1)] and use quasi-neutrality condition to derive the mode structure equation.

We consider only electrostatic perturbations and do not perturb the magnetic field [Ossakow and Chaturvedi, 1979]. By perturbing Eq. (2) for both electrons and ions, we obtain the perturbed velocities in the z direction

$$\hat{V}_{ez} = -\frac{e\,\hat{E}_z}{m_e \nu_{ei}} \tag{7}$$

$$\hat{V}_{iz} = 0 \tag{8}$$

The perpendicular perturbed velocities are given as

$$\hat{V}_{e\perp} = \frac{c}{B}\left[\hat{E}_\perp \times \hat{z} - \left(\nu_{ei}/\Omega_e\right)\hat{E}_\perp\right] \tag{9}$$

$$\hat{V}_{i\perp} = \frac{c}{B}\left[\hat{E}_\perp \times \hat{z} - i\,\frac{\left(\omega + i\nu_{in}\right)}{\Omega_i}\,\hat{E}_\perp\right] \tag{10}$$

We substitute Eqs. (7)-(10) in Eq. (1) and use $\underline{E} = -\nabla\phi$ in the electrostatic limit. Then we subtract the electron continuity equation from the ion continuity equation and impose quasineutrality to obtain

$$\frac{\partial^2\hat{\phi}}{\partial x^2} + p(x)\,\frac{\partial\hat{\phi}}{\partial x} + q(x)\hat{\phi} = 0, \tag{11}$$

where

$$p(x) = n_o'/n_o \tag{12}$$

$$q(x) = -k_y^2 - \frac{i\,k_z^2\left(\Omega_e/\nu_{ei}\right)\Omega_i}{\left(\omega + i\nu_{in}\right)}$$

$$+ \frac{k_z V_d(x)}{\left(\omega - k_z V_d(x)\right)}\,\frac{\Omega_i}{\left(\omega + i\nu_{in}\right)}\left[k_y\left(n_o'/n_o\right) - i\left(\Omega_e/\nu_{ei}\right)k_z^2\right] \tag{13}$$

This equation agrees with the nonlocal mode structure equation derived earlier by Satyanarayana and Ossakow (1984) and Huba (1984).

The effects of finite current width are contained in the third term in Eq. (13). We solve Eq. (11) exactly for two specific profiles of the

current velocity $V_d(x)$. In the next section, we obtain the analytic dispersion relation for a "waterbag" distribution.

$$V_d(x) = \begin{cases} \bar{V}_d, & |x| \leq d \\ 0, & |x| > d \end{cases} \tag{14}$$

where 2d is the current channel width. We choose an exponential plasma density profile $n_o(x) = \bar{n}_o \exp(x/L)$ so that $n_o'/n_o = 1/L$. In section IV we present the numerical results for both the waterbag current model and the diffuse Gaussian current model.

III. DISPERSION RELATION

The dispersion relation is obtained by matching the logarithmic derivatives of the wavefunction inside and outside the waterbag at the boundaries, $x = \pm d$, and requiring that the solution be evanescent for $x \to \pm \infty$. First, we will cast Eq. (11) into a Schrodinger type equation by using the transformation

$$\hat{\phi} = \psi(x) \exp\left[-\frac{1}{2}\int p(x)dx\right]. \tag{15}$$

Then, we have

$$\frac{\partial^2\psi}{\partial x^2} + Q^2(x)\,\psi = 0 \tag{16}$$

where

$$Q^2(x) = q(x) - p^2/4 - p'/2 \tag{17}$$

and $p' = \partial p/\partial x$. For an exponential density profile, $n_o = \bar{n}_o \exp(x/L)$, $p = 1/L$ and $p' = 0$. Thus, for the waterbag profile $V_d(x)$ given by Eq. (14) and for the exponential density profile, Eq. (16) can be written as

$$\frac{\partial^2\psi_{out}}{\partial x^2} - Q_o^2\,\psi_{out} = 0 \qquad |x| > d \tag{18}$$

$$\frac{\partial^2\psi_{in}}{\partial x^2} + Q_i^2\,\psi_{in} = 0 \qquad |x| \leq d \tag{19}$$

with

$$Q_i^2 = -\left[k_y^2 + 1/\left(4L^2\right)\right] - \frac{i\,k_z^2\left(\Omega_e/\nu_{ei}\right)\Omega_i}{\left(\omega + i\nu_{in}\right)}$$

$$+ \frac{k_z\,\bar{V}_d}{\left(\omega - k_z\bar{V}_d\right)}\,\frac{\Omega_i}{\left(\omega + i\nu_{in}\right)}\left[k_y/L - i\,k_z^2\left(\Omega_e/\nu_{ei}\right)\right] \tag{20}$$

and

$$Q_o^2 = \left[k_y^2 + 1/\left(4L^2\right)\right] + \frac{i\,k_z^2\left(\Omega_e/\nu_{ei}\right)\Omega_i}{\left(\omega + i\nu_{in}\right)} \tag{21}$$

where primes indicate derivatives with respect to x. The current convective instability is a nearly purely growing mode with $\omega = \omega_r + i\gamma \sim i\gamma$. This will be shown to be true <u>a posteriori</u> in the next section. For $\omega_r < \gamma$, the sign convention applicable in Eqs. (18) and (19) is such that $Q_o^2 > 0$ and $Q_i^2 > 0$. In Eq. (20) the sign of $\bar{V}_d/L$ (< 0) is chosen so that $Q_i^2 > 0$ and the growth rate is positive for positive k_y. Furthermore, in the following we assume that $|k_z\bar{V}_d| \ll |\omega|$ in the denominator and $k_z^2\left(\Omega_e/\nu_{ei}\right) < k_y/L$. First, we rewrite Q_i^2 and Q_o^2 as follows:

$$\hat{Q}_o^2 = \frac{\hat{k}^2\left(\omega + i\bar{\nu}\right)}{\left(\omega + i\nu_{in}\right)} \tag{22}$$

$$\hat{Q}_i^2 = -\frac{\hat{k}^2\left(\omega - \omega_+\right)\left(\omega - \omega_-\right)}{\omega\left(\omega + i\nu_{in}\right)} \tag{23}$$

where

$$\bar{\nu} = \nu_{in} + \left(\hat{k}_z^2/\hat{k}^2\right)\left(\Omega_e/\nu_{ei}\right)\Omega_i \tag{24}$$

$$\omega_o^2 = \omega_+\omega_- = \left(\hat{k}_z\hat{k}_y/\hat{k}^2\right)\left|\bar{V}_d/L\right|\Omega_i \tag{25}$$

$$\omega_\pm = -\left(i\bar{\nu}/2\right)\left[1 \pm \left(1 + 4\left(\omega_o^2/\bar{\nu}^2\right)\right)^{1/2}\right] \tag{26}$$

$$\hat{k}^2 = \hat{k}_y^2 + 1/4 \tag{27}$$

and $\hat{k}_y$, $\hat{k}_z$, and $\hat{d}$ are the normalized quantities k_yL, k_zL, and d/L respectively. We note that $\omega_\pm$ are the two roots of the local dispersion relation $[Q_i = 0]$. Since the potential, $\hat{Q}_i^2(x)$, in Eq. (16) is symmetric about $x = 0$, we can restrict our analysis to eigenfunctions of definite parity.

In the region $|x| < d$ we have

$$\psi_{in} = A \cos [\hat{Q}_i x/L] \qquad \text{for even parity} \tag{28}$$

$$\psi_{in} = B \sin [\hat{Q}_i x/L] \qquad \text{for odd parity} \tag{29}$$

where A and B are constants. In the region $|x| > d$, we have an exponentially decreasing solution for either case

$$\psi_{out} = C\, e^{-\hat{Q}_o|\frac{x}{L}|} \tag{30}$$

where C is a constant. The matching condition in the case where $V_{iz}^0 = 0$ is that the logarithmic derivative be continuous at $x = \pm d$

$$[\psi'_{in}/\psi_{in}]_{d_-} = [\psi'_{out}/\psi_{out}]_{d_+}$$

where $d_\pm = \lim_{\varepsilon \to o}[d \pm \varepsilon]$. This condition yields the dispersion relation

$$\hat{Q}_i \tan [\hat{Q}_i \hat{d}] = \hat{Q}_o \qquad \text{even modes} \tag{31a}$$

$$\hat{Q}_i \operatorname{cotan} [\hat{Q}_i \hat{d}] = -\hat{Q}_o \qquad \text{odd modes} \tag{31b}$$

The effect of finite current channel width are contained in the argument of the tangent (cotangent) function for the even modes (odd modes). We analyze the dispersion relation for the even modes by first inverting Eq. (31a) to obtain

$$\hat{Q}_i = \frac{1}{\hat{d}} [\text{Arc tan } [\hat{Q}_o/\hat{Q}_i]] \tag{32}$$

We can rewrite Eq. (32) as

$$\hat{Q}_i = \frac{1}{d}\left[\tan^{-1}\{\hat{Q}_o/\hat{Q}_i\} + m\pi\right] \tag{33}$$

where $\tan^{-1}\{\hat{Q}_o/\hat{Q}_i\}$ is the principal value of Arc $\tan\{\hat{Q}_o/\hat{Q}_i\}$ and m is an integer. Equation (33) is the fundamental nonlocal dispersion relation. We note that when d = 0, the dispersion relation $Q_o = 0$ from Eq. (31a) does not give instability since the currents driving the instability vanish.

We can compare Eq. (33) and Eq. (19) to understand the local and nonlocal limits. We recall that the local limit means that the current channel width is infinite so that Eq. (19) describes the mode structure throughout the space. In the local theory, Eq. (19) is also Fourier analyzed with respect to x to obtain

$$Q_i^2 = k_x^2 \tag{34}$$

and if we assume $k_y^2 >> k_x^2$ we regain the earlier results of Ossakow and Chaturvedi (1979), $\hat{Q}_i \sim 0$, corresponding to $\omega \sim \omega_\pm$. Comparing Eqs. (33) and (34) we see that in the nonlocal analysis, the right hand side of Eq. (33) provides the inverse scale length, L_x^{-1}. The role played by the current channel, then, is to form a wavepacket of width of the order of L_x localized within the current channel.

In the limit $|\hat{Q}_o/\hat{Q}_i| >> 1$, $\tan^{-1}\{Q_o/Q_i\}$ approaches $\pi/2$. This happens in the local limit when $\omega \simeq \omega_\pm$ as can be seen by dividing Eq. (22) by Eq. (23) to obtain

$$\frac{\hat{Q}_o^2}{\hat{Q}_i^2} = -\frac{\omega(\omega + i\bar{\nu})}{(\omega - \omega_+)(\omega - \omega_-)}$$

As we approach the local limit we have from Eq. (33)

$$\hat{Q}_i = (m + 1/2)\pi/d \tag{35}$$

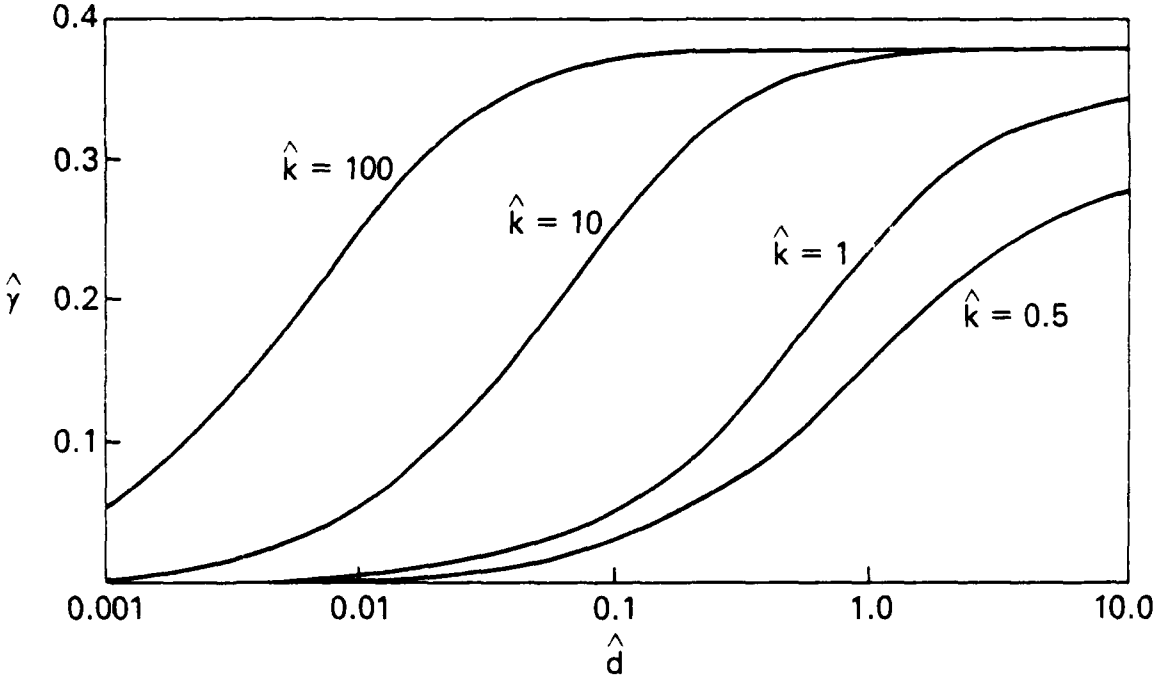

Figure 4

Plot of growth rate $\hat{\gamma}$ versus wavenumber $\hat{k}$ in the collisional limit for diffuse boundary case. The profiles used for the current and the density are given in Eqs. (53) and (54), respectively. The parameters used are the same as in Fig. 3.

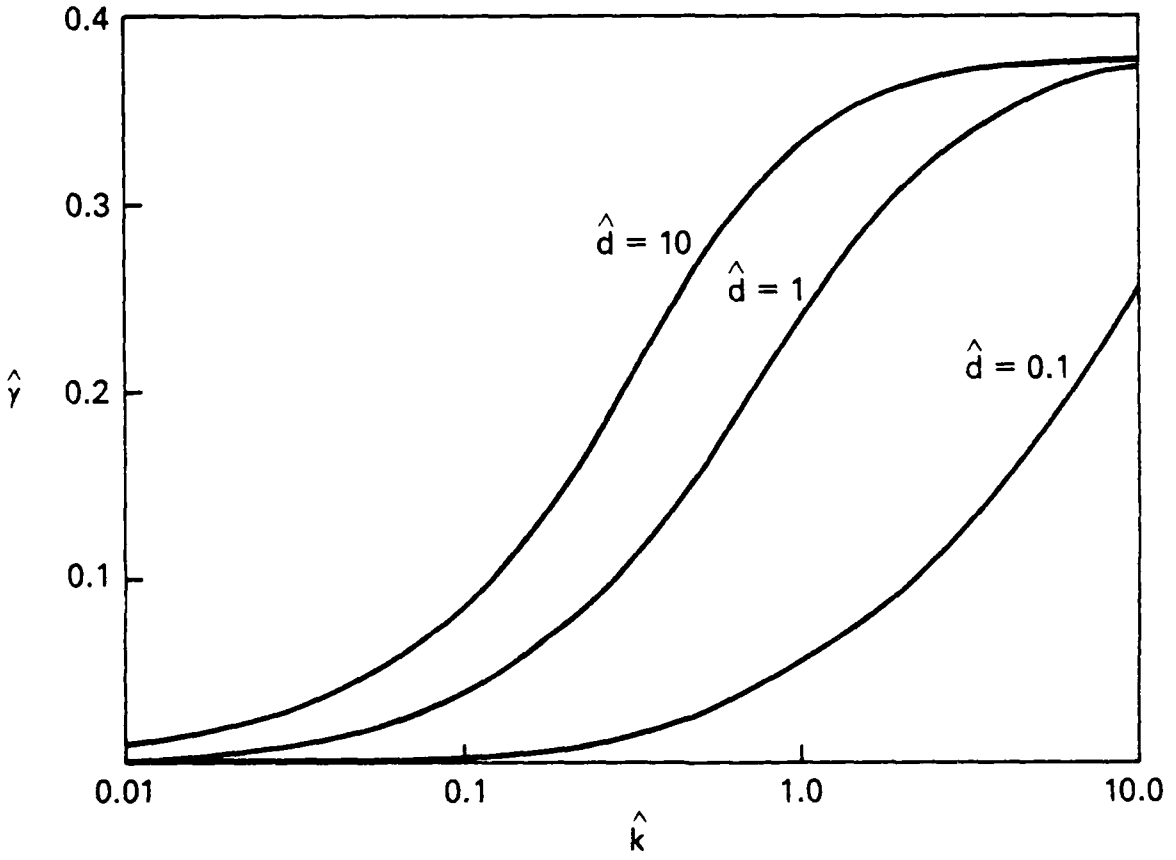

Figure 3

Plot of growth rate $\hat{\gamma}$ versus $\hat{k}$ for $\hat{d} = 0.1$, 1.0, and 10.0 for sharp boundary case. The parameters chosen are $\nu_{in}/|\bar{V}_d/L| = 1$, $\Omega_i/|\bar{V}_d/L| = 10^4$, and $\nu_{ei}/|\bar{V}_d/L| = 10^{-4}$.

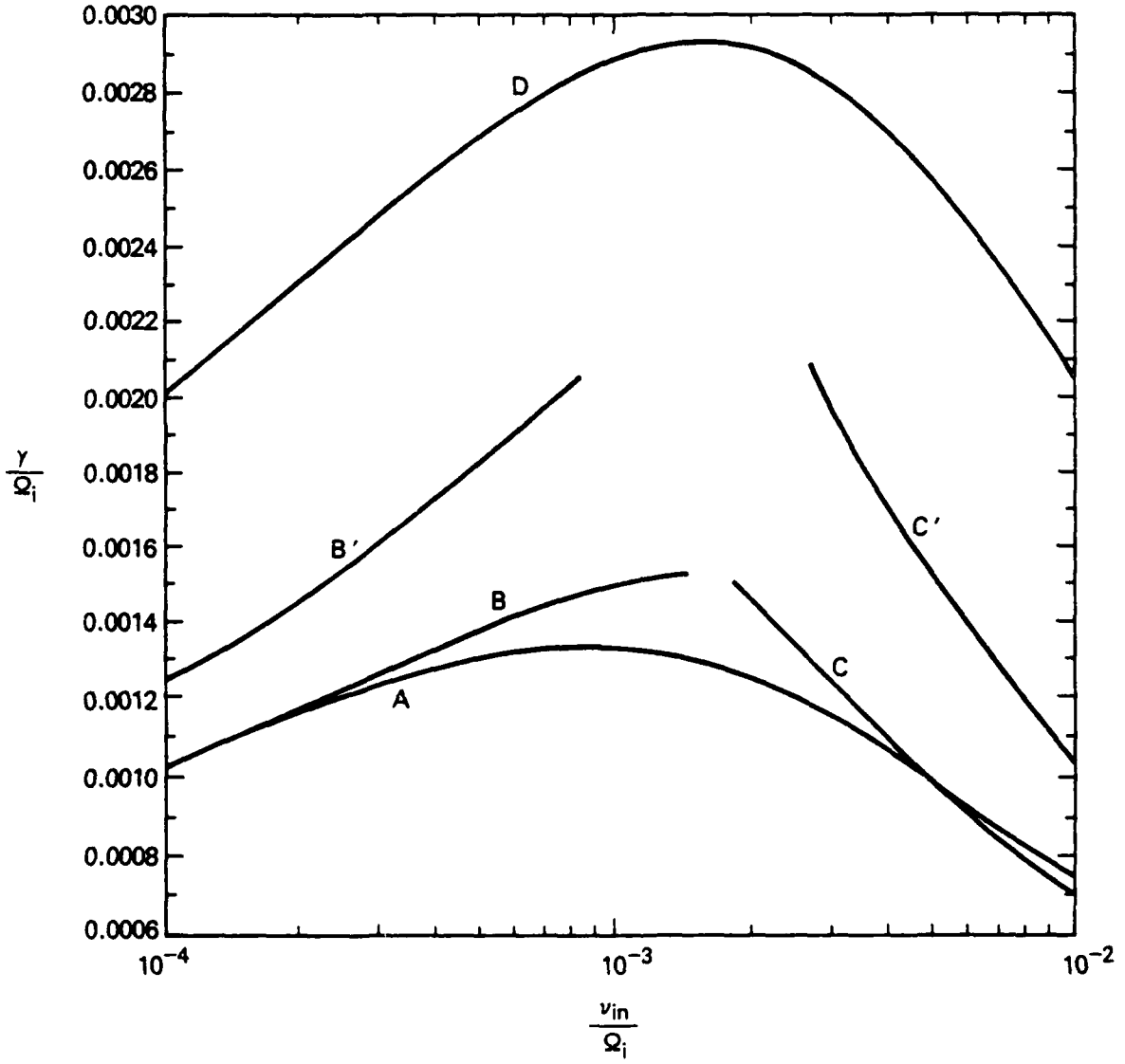

Figure 2

Plot of growth rate (γ/Ω_i) versus the ion-neutral collision frequency (ν_{in}/Ω_i) for $k_y d = 0.3$, $\hat{V}_d/L = 5.0$, and $\nu_{ei}/\Omega_e = 10^{-4}$. Curve A shows the exact numerical solutions of Eq. (33). Curves B and C represent Eqs. (46) and (42) which are solutions in the inertial and collisional limits for long wavelength modes. Curves B′ and C′ represent the simplified analytical expressions, Eqs. (52) and (43), in the same limits. Curve D is the local solution, ω_-, given by Eq. (38).

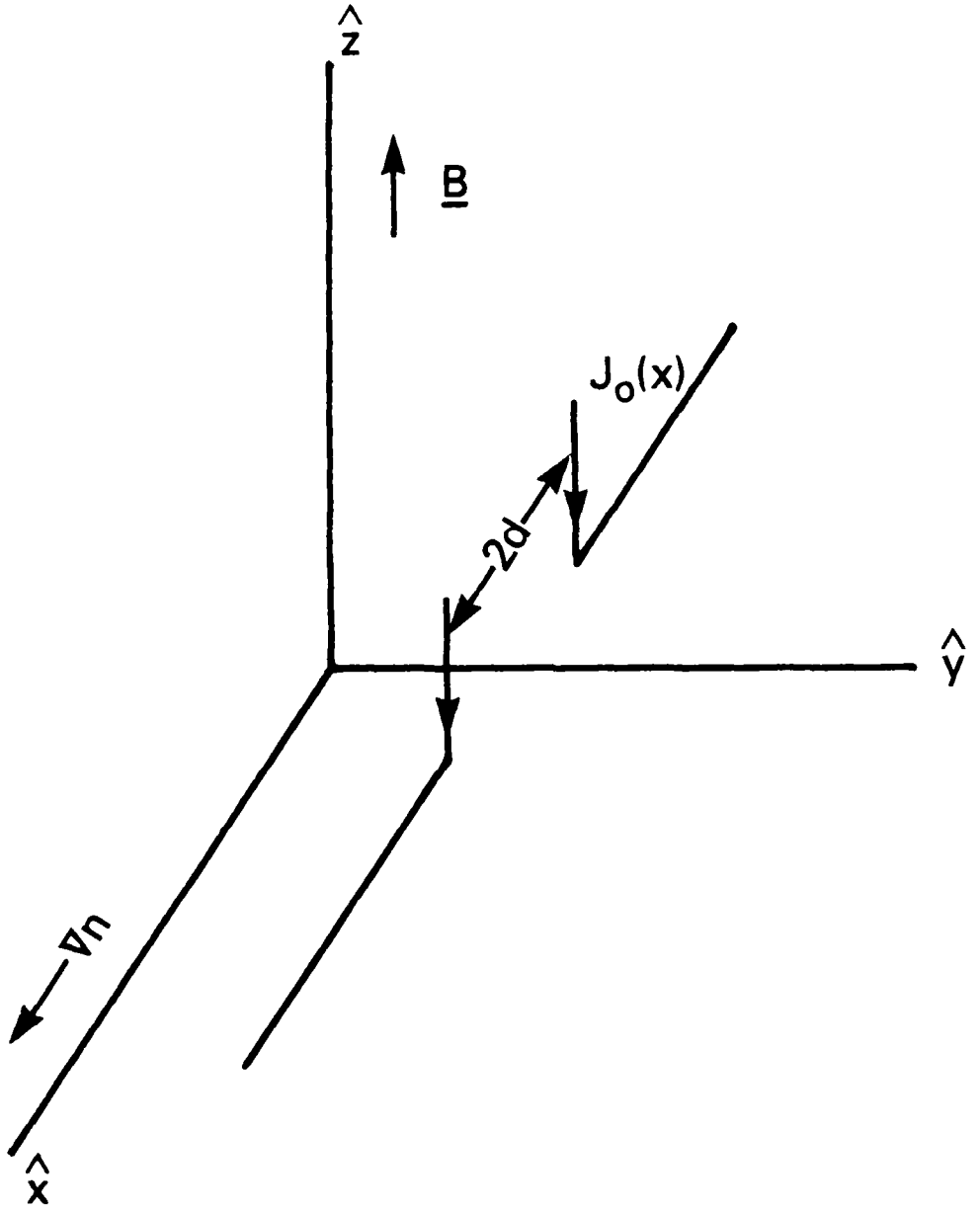

Figure 1

Schematic of the geometry used displaying the finite current channel of width 2d along $\hat{x}$.

ACKNOWLEDGMENTS

We would like to thank J. Huba for the critical reading and suggestions for improvement of the manuscript and G. Ganguli, Y.C. Lee, P. Chaturvedi, and S.L. Ossakow for constructive discussions. This work has been supported by the Office of Naval Research and the Defense Nuclear Agency.

that both the long and short wavelength modes driven by the current convective instability should have longer growth times than previously estimated. Other data sets have also shown very narrow high latitude F-region field-aligned currents. From the results of this paper, we expect the nonlocal nature to have an important impact.

Recently Bythrow et al. (1984) using HILAT satellite data have measured very large downward currents (~ 100 $\mu A/m^2$), presumably carried by cold upward drifting electrons, in the high latitude topside F-region ionosphere. The dimensions of these currents perpendicular to the magnetic field is of order the transverse scale size (~ 3 km) of precipitation induced density structures. Turbulent horizontal ion drifts were also measured in conjunction with the large currents and transverse density gradients. Their data shows that d ~ 1.9 km, L = 6 km, and $\bar{V}_d$ = 30 km/sec. In the case of ionospheric F region, $\nu_{ei}/\Omega_e \sim 10^{-4}$ and $\nu_n/\Omega_i \sim 10^{-3}$. For these parameters Eq. (33) yields the growth rates as $\gamma \sim 0.0028\ \Omega_i$, $0.0026\Omega_i$, and $0.00146_i\Omega$, for λ = 1, 2, and 10 km, respectively. Whereas, for d/L >> 1, the local growth rate is ~ $0.0031\ \Omega_i$. For narrower current channel and large density gradients or longer wavelength modes the growth rate could be substantially lower.

Finally, several aspects of the theory of the effects of finite current channel width on the current convective instability have not been discussed here. For very large currents, the self-consistent role of magnetic shear must be included [Huba and Ossakow, 1980]. An approximate value of the scale length for magnetic shear is $L_s \approx cB/4\pi J$ with c, the speed of light, B the magnetic field, and J the current density. For $J \approx 10^{-6} A/m^2$ and B ~ 0.5 G we find $L_s \sim 10^4$ km. For $d \ll L_s$ where d is the current channel width we do not expect magnetic shear effects to play an important role. In addition, we have not considered self-consistent velocity shear and its effects on the current convective instability with a finite current channel width, the finite parallel extent of the auroral ionosphere, electromagnetic effects, or nonlinear aspects. We are presently investigating several of these aforementioned effects.

total integrated currents in order to predict the behaviour of the plasma at any point. Second, because there is no plane wave in the x direction, an observer passing through the current channel in the x direction does not see the usual Doppler shift $k_x V_o$ that would be predicted by a local theory, where V_o is the velocity of the observer. This point has also been noted by Ganguli et al. (1984) in connection with the current driven ion cyclotron instability. The two perpendicular directions, x and y, are no longer equivalent.

The wavefunction as given by Eqs. (21) and (30) shows that it is localized around the point $x = 0$ with a width $L_x \approx 1/\theta_i$ given by Eq. (33). The fastest growing mode ($m = 0$) has a single peak around $x = 0$. Note that the width of the wave packet is directly proportional to d, which implies that in the presence of wider channels the wavefunction is spread out, whereas in the presence of narrow channels the wavefunction is sharply peaked.

An important result is that in the long wavelength limit, the growth rate scales as some power of the product of the magnitude of the drift velocity and the current channel width $(\overline{V}_d d/L^2)^\alpha$, $\alpha \leq 1$. This suggests that the growth rate would be the same whether a weaker current is distributed over a larger channel or a stronger current is concentrated in a narrow channel. With regard to the auroral ionosphere, if the density gradient scale length is around 20 kms, then we see from Fig. 4, that the growth rate of smaller scale modes, say $\lambda \sim 1$ km corresponding to $k_y L \sim 100$, is reduced from $0.3\ \overline{V}_d/L$ to $0.15\ \overline{V}_d/L$ by a current channel of width $2d = 40$ km. The above growth rate corresponds to $0.75\ 10^{-3}\ s^{-1}$ if $\overline{V}_d = 50$ m/s (corresponding to currents of order $\mu A/m^2$). Since $\nu_{in} \sim \overline{V}_d/L$, these parameters correspond to the high latitude F region. We also point out that the short wavelength modes ($k_y L < 1$) are not affected by the current channels of 40 kms width.

Vickrey et al. (1980) have computed the growth rates from the current convective instability to explain small scale plasma density fluctuations near high latitude F region large scale plasma enhancements. However, their data indicate that the transverse dimensions of the currents driving the instability are comparable to the perpendicular (to the geomagnetic field) scale sizes of the plasma enhancements. Our results suggest that their growth rates are overestimates. From our analysis we would predict

V. DISCUSSION AND SUMMARY

We have presented an analysis of the effects of finite current channel width on the current convective instability. The current convective instability results from the coupling of a magnetic field aligned current and a density gradient perpendicular to the magnetic field in the presence of electron-neutral collisions. For a current with perpendicular scale size 2d and a plasma density gradient scale length L, our analytical results indicate a monotonic decrease in the growth rate γ of the current convective instability for $d/L < 1$ both in the collisional $(\nu_{in} >> \omega)$ and inertial limits $(\nu_{in} << \omega)$. For $d/L << 1$, we find $\gamma \propto \bar{V}_d d/L^2$ in the collisional limit while $\gamma \propto (\hat{V}_d d/L^2)^{\alpha}$, $\alpha < 1$ in the inertial limit. In general, the growth rate of the current convective instability is reduced by the finite width of the current channel from that of the local case in which the current distribution is infinite in extent.

It is significant to note that, in the long wavelength limit $k_y d << 1$ where the nonlocal effects are most prominent, the dependence on $V_d(x)$ enters the nonlocal results in the sharp-boundary case in the form of $(\bar{V}_d d)$, the "area" under the function $V_d(x)$ in the current channel. It is clear that this quantity is proportional to the total current in the channel per unit length in the y-direction (divided by the density of the current carriers and the electric charge). This point is to be contrasted with the local dispersion relation (34) in which the growth rate depends on the current velocity itself, a local quantity. In addition, the nonlocal growth rate depends on the fractional plasma density gradient across the current channel (i.e. d/L). The growth rate is reduced because in a growth period $(\sim (V_d/L)^{-1})$ the fluid element does not sample the entire gradient (1/L) but a smaller fraction of the density gradient (f/L , f = d/L). Furthermore, a single value of γ corresponds to the entire wavepacket which occupies the current channel. These nonlocal features are well-known and general to all intrinsically nonlocal perturbations such as the tearing mode (see, for example, Chen and Palmadesso, 1984). With respect to perturbations that have valid local limits, certain differences in the interpretation of theoretical and observational results must be kept in mind as one goes from the local to nonlocal regime. First, with finite current channels, observations must provide global quantities such as the

50%. Furthermore, we notice that the longer wavelength modes are more easily stabilized. That is, a wider channel ($\hat{d} \gtrsim 10$) significantly reduces the growth rate of modes with wavelength of $4\pi L$ ($\hat{k} = 0.5$), whereas channel width of $\hat{d} = 0.1$ reduces the growth rate of modes with wavelengths of $0.2\pi L$($\hat{k} = 10$) by the same amount. From figures 3 and 4, we can conclude that the growth rate of the current convective instability is reduced if the current channel width is such that $kd \lesssim 1$. Similar results were noticed in the context of collisionless current driven ion-cyclotron waves by Bakshi et al. (1983). We note that we find the real part of the frequency to be much smaller than the growth rate, $\hat{\omega}_r \sim 10^{-4} << \hat{\gamma}$.

We have also numerically solved equation (11) for a more realistic diffuse profile of density and current. We choose a density profile given by

$$n(x) = n_o \frac{1 + \varepsilon \tanh (x/L)}{1 - \varepsilon} \tag{53}$$

so that

$$\frac{n'}{n} = \frac{1}{L} \frac{\varepsilon \operatorname{sech}^2(x/L)}{1 + \varepsilon \tanh (x/L)}$$

We take $\varepsilon = 0.8$ so that n'/n is a maximum at $x/L \equiv x_o = -0.55$. We find then that $(n'/n)_{max} = 1/L$. In addition we consider a smooth profile for the current velocity $V_d(x)\hat{z}$ with

$$V_d(x) = \overline{V}_d \exp\left[-(x-x_o)^2/d^2\right] \tag{54}$$

We take the same parameters as in the sharp boundary case. In Fig. 5 we plot $\hat{\gamma}$ versus $k_y L$ for several values of d/L. Similar nonlocal behavior is seen for the growth rate $\hat{\gamma}$. In Fig. 6, we plot $\hat{\gamma}$ versus d/L. The results shown in these figures are similar to those obtained by using a simple waterbag model (Figs. 3 and 4) leading us to believe that the simple waterbag model adequately models the essential physics, namely that the finite current channel width has a stabilizing influence on the current convective instability.

is that for $d << \lambda$ the growth rate scales as $[V_d d/L^2]^\alpha$, where $\alpha < 1$. This result shows that in the long wavelength limit the growth rate depends on the total current in the region where the wave packet is localized rather than on V_d as is true in the local case.

In solving equation (33), we consider the fastest growing mode ($m = 0$) and use the following parameter values: $\nu_{in}/|\bar{V}_d/L| = 1$, $\Omega_i/|\bar{V}_d/L| = 10^4$, $\nu_{ei}/\Omega_e = 10^{-4}$ and $k_z/k_y = [\nu_{ei}\nu_{in}/\Omega_e\Omega_i]$ (Chaturvedi and Ossakow, 1981; Satyanarayana and Ossakow, 1984). In Fig. 3, we plot the normalized growth rate $\hat{\gamma} \equiv \gamma/|\bar{V}_d/L|$ as a function of $\hat{k} = k_y L$ for various values of the width of the current channel normalized to density gradient scale length $\hat{d} \equiv d/L$ = 0.1, 1.0, and 10.0. First, we see the nonlocal behaviour of the instability where the growth rate is reduced for $\hat{k} \equiv k_y L < 1$ and slowly increases and saturates to the local limit at $\hat{k} >> 1$ (Huba, 1984). Second, the larger the value of $\hat{d}$, the smaller is the $\hat{k}$ value for which the local limit $\hat{\gamma}_L$ is achieved; for $\hat{d} = 10$, $\hat{\gamma}$ approaches $\hat{\gamma}_L$ for $\hat{k} \gtrsim 2$ whereas for $\hat{d} = 0.1$, $\hat{\gamma}$ approaches $\hat{\gamma}_L$ for $\hat{k} \sim 100$(not shown in figure). The local limit, $\hat{\gamma}_L$, is given by the imaginary part of Eq. (38) normalized to $|\bar{V}_d/L|$. Thus we can conclude that the current channel width has be to small ($\hat{d} \lesssim 1$) to substantially reduce the growth rate of the short wavelength modes ($\hat{k} > 1$).

In Figure 4 we plot $\hat{\gamma}$ as a function of $\hat{d}$ for $\hat{k}$ = 0.5, 1.0, 10.0, and 100.0. As we discussed earlier, we see that as $\hat{d} \to \infty$ we recover the conventional current convective growth rate ($\hat{\gamma}_L$ given in Eq. (38)). The second point is that, as $\hat{d}$ is decreased, the growth rate decreases, eventually going to zero for $\hat{d} \to 0$. The quenching of the instability should be expected, because as $\hat{d} \to 0$ the currents that are driving the current convective instability become highly localized and thus do not sample the entire density gradient. Since the instability is driven by the density gradient in the presence of field aligned currents, as the current channel width (d) is reduced in relation to the density gradient scale length (L), the growth rate of the instability is reduced. The instability is most sensitive to the finite width of the current channel when the current channel width, d, is comparable to or less than the gradient scale length, L. In fact, when the wavelength is comparable to the current channel width, $\lambda \sim d$ implying $kd \sim 2\pi$, the growth rate drops by at least

In this limit where $|Q_o/Q_i| \ll 1$, $\nu_{in} \ll |\omega|$ and $k_{zl}^2 \nu_{in} \ll |\omega|$, the growth rate depends on the square root of the product of $\bar{V}_d$ and d. An important conclusion is that in both limits discussed above the growth rate scales as $\{\bar{V}_d d/L^2\}^{\alpha}$, $\alpha \leq 1$. We note that the growth rates given in Eqs. (42)-(46) can be shown to be less than the local growth rate, $|\omega_+|$, as assumed earlier. In the next section we solve numerically the full nonlocal dispersion relation [Eq. (33)] in order to study the growth rate over a larger range of $k_y L$ and d/L.

IV. NUMERICAL RESULTS

In order to illustrate the properties of Eq. (33) and the scaling properties of the growth rate in the collisional and inertial domains, we have chosen, for convenience, the case where $k_{zl} = 1$. This choice corresponds to $k_z = k_y(\nu_{ei}/\Omega_e)(\nu_{in}/\Omega_i) \ll k_y$. With this choice, the local dispersion relation (equation (38)) exhibits a maximum at $\nu_{in}/\Omega_i = (1/24)^{2/3} (\omega_o^2/\Omega_i^2)^{2/3}$. This is shown in Fig. 2 where we plot γ/Ω_i versus ν_{in}/Ω_i. As a numerical example, we choose $\nu_{ei}/\Omega_e = 10^{-4}$, $|\bar{V}_d/L| = 5$, $d/L = 0.3$ and $k_y L = 1$ (Bythrow et al., 1984). Curve A shows the exact solution of Eq. (33) obtained by solving it numerically. Curves B and C represent the growth rates given by the analytical expressions in Eqs. (46) and Eq. (42) in the inertial and collisional domains, respectively. These curves show that there is good agreement between the numerical results and the analytical expressions given in Eqs. (42) and (46). Curves B′ and C′ show the simplified analytical expressions given by Eqs. (43) and Eq. (52). Curve D gives the local growth rate, ω_-, given by Eq. (38). The figure shows that for small current channel widths, $d \sim 0.3\,\lambda/2\pi$, where λ is the wavelength of the perturbation, the growth rate is reduced by an order of magnitude. For the particular choice of the parallel wavenumber the growth rate peaks at $\nu_{in}/\Omega_i \sim 2.0\ 10^{-3}$ whereas it is maximized at $\nu_{in}/\Omega_i \sim 5.0\ 10^{-3}$ in the nonlocal limit. In addition, curves B′ and C′ show that the Eqs. (43) and (52), which contain the scaling properties of the growth rate, agree fairly well with the exact numerical results in $\nu_{in} \gg \Omega_i$ and $\nu_{in} \ll \Omega_i$ regimes, respectively. Based on this agreement we can say that the growth rate scales as $\{\nu_{in}/\Omega_i\}^{1/2}$ in the collisional domain and as $\{\nu_{in}/\Omega_i\}^{-1/2}$ in the inertial limit. A more important result

Inertial limit

In the inertial limit where $\nu_{in} << |\omega|$, the solutions of Eq. (41) are

$$\omega_{<} = -\{i\nu_{<}/2\} \{1 \pm \{1 + 4\,\omega_o^2\,\{1 + \kappa_2\}/\nu_{<}^2\}^{1/2}\}/\{1 + \kappa_2\} \tag{46}$$

where $\kappa_2 = \{1/k_y d\}$ and $\nu_{<} = \bar{\nu} + \nu_{in}\hat{k}_{z1}^2\kappa_2^2/2$. To obtain a simple expression for the growth rate, we consider small channel widths, (d << L), where the growth rate is much smaller than the local growth rate. Thus for $\omega << \omega_{\pm}$ Eq. (40) yields in the inertial limit

$$\omega_+\omega_-\hat{k}\hat{d} = -\omega^2\{1 + i\hat{k}_{z1}^2\nu_{in}/\omega\}^{1/2} \tag{47}$$

Equation (47) can be simplified for the case $\hat{k}_{z1}^2\ \nu_{in} >> |\omega|$, i.e., $\{\hat{k}_z^2/\hat{k}^2\}\{\Omega_e/\nu_{ei}\} >> |\omega|/\Omega_i$. The growth rate can then be written as

$$\gamma = \{\nu_{ei}\Omega_i/\Omega_e\}^{1/3}\{\hat{k}_y\hat{d}\}^{2/3}\{|\bar{V}_d|/L\}^{2/3} \tag{48}$$

From Chaturvedi and Ossakow, (1981) we have, in the local inertial limit the maximum growth rate

$$\gamma_L = \{\nu_{ei}\Omega_i/\Omega_e\}^{1/3}\{|\bar{V}_d|/L\}^{2/3} \tag{49}$$

As a result, we have for the nonlocal long wavelength inertial limit,

$$\gamma = \{k_y d\}^{2/3}\gamma_L \tag{50}$$

Equation (50) shows that the nonlocal growth rate in the inertial limit γ is less than the local growth rate since $k_y d << 1$ in the long wavelength limit. For $k_{z1}^2\nu_{in} << |\omega|$, i.e., $\{\hat{k}_z^2/\hat{k}^2\}\{\Omega_e/\nu_{ei}\} << |\omega|/\Omega_i$, Eq. (47) yields

$$\gamma = \{\omega_+\omega_-\hat{k}\hat{d}\}^{1/2} \tag{51}$$

By using Eqs. (24) - (27), this expression can be rewritten as

$$\gamma = \{\hat{k}_z\hat{k}_y/\hat{k}\}^{1/2}\{\Omega_i\}^{1/2}\{|\bar{V}_d/L|\}^{1/2}(d/L)^{1/2} \tag{52}$$

Collisional limit

In this limit where $\nu_{in} >> |\omega|$, Eq.(41) has the following roots:

$$\omega_> = -\{i\nu_>/2\} \{1 \pm \{1 + 4\,\omega_o^2\,\{1 + \kappa_1\}/\nu_>^2\}^{1/2}\}/\{1 + \kappa_1\} \tag{42}$$

where $\kappa_1 = \{1 + \hat{k}_{z1}^2\}^{1/2}/k_y d$ and $\nu_> = \nu + \nu_{in}\kappa_1$. A simple expression for the growth rate can be obtained by examining the small channel width limit, d << L, where the growth rate is much less than the local growth rate. Thus for $\omega << \omega_{\pm}$, Eq. (40) or (41) yields

$$\omega_+\omega_-\hat{k}\hat{d} = - i\omega\nu_{in}\{1 + \hat{k}_{z1}^2\}^{1/2}$$

from which the growth rate $\{\omega = \omega_r + i\gamma\}$ is given as

$$\gamma = \{\hat{k}_z\hat{k}_y/\hat{k}\}\{1 + \hat{k}_{z1}^2\}^{-1/2}\{\Omega_i/\nu_{in}\}\,|\bar{V}_d/L|\,(d/L) \tag{43}$$

It is worthwhile to compare the growth rate in nonlocal long wavelength limit as given by Eq. (43) with the local result as given by Chaturvedi and Ossakow, (1981)

$$\gamma_L = \{k_z/k_y\}\{\Omega_i/\nu_{in}\}\{\bar{V}_d/L\}\{1 + \hat{k}_{z1}^2\}^{-1} \tag{44}$$

We then find the simple result

$$\gamma = k_y d\{1 + \hat{k}_{z1}^2\}^{1/2}\gamma_L \tag{45}$$

Since $k_y d < 1$ in the nonlocal long wavelength limit, the nonlocal growth rate is less than the local growth rate. Several important conclusions can be drawn from this nonlocal analysis. In this collisional long wavelength limit, (i) the growth rate depends on the product of the magnitude of the drift velocity, $\bar{V}_d$, and the current channel width, d; (ii) the growth rate scales inversely with ν_{in}, the ion-neutral collision frequency; and (iii), the growth rate scales inversely with the gradient scale length, L.

We set m = 0 and consider the fastest growing mode. Then, with the definition of $\hat{Q}_i$ from Eq. (23), Eq. (35) becomes

$$- \hat{k}^2 \frac{(1 - \omega_+/\omega)(1 - \omega_-/\omega)}{(1 + i\nu_{in}/\omega)} = \frac{\pi^2}{4\hat{d}^2} \tag{36}$$

Thus, as we approach the local limit, we have $L_x = 2d/\pi$ and L_x plays the role of the wavelength in the x direction. For $\nu_{in}/|\omega| << 1$ the new roots are

$$\omega = \frac{- (i\bar{\nu}/2) \left[1 \pm \left[1 + 4\, \omega_o^2\, (1 + \pi^2/4\hat{k}^2\hat{d}^2)/\bar{\nu}^2\right]^{1/2}\right]}{(1 + \pi^2/4\hat{k}^2\hat{d}^2)} \tag{37}$$

Furthermore, we regain the local growth rates for $k_y d \to \infty$, namely,

$$\omega \equiv \omega_{\pm} = (-i\bar{\nu}/2)\left[1 \pm \left[1 + 4(\omega_o^2/\bar{\nu}^2)\right]^{1/2}\right] \tag{38}$$

In the limit $|\hat{Q}_o/\hat{Q}_i| << 1$, the inverse tangent function is approximately equal to $\hat{Q}_o/\hat{Q}_i$. Then Eq. (33) becomes

$$\hat{Q}_o/\hat{Q}_i = \hat{Q}_i\, \hat{d} \tag{39}$$

Using Eqs. (22) and (23) we obtain

$$(\omega - \omega_+)(\omega - \omega_-) = - \omega(\omega + i\nu_{in})\left[1 + i\hat{k}_{z1}^2 \nu_{in}/(\omega + i\nu_{in})\right]^{1/2}/\hat{k}\hat{d} \tag{40}$$

where $\hat{k}_{z1}^2 = (\hat{k}_z^2/\hat{k}^2)(\Omega_e/\nu_{ei})(\Omega_i/\nu_{in})$. The above equation is valid for $(\hat{Q}_o/\hat{Q}_i) << 1$ or $|\hat{Q}_i \hat{d}| << 1$ which is essentially the long wavelength limit, $k_y d << 1$. Equation (40) can then be solved both in the highly collisional and weakly collisional domains. Using Eqs. (24) and (25), Eq. (40) can be written as

$$\omega^2 + i\bar{\nu}\, \omega + \omega_o^2 \approx \pm\, \omega(\omega + i\nu_{in})\left[1 + i\, \hat{k}_{z1}^2 \nu_{in}/(\omega + i\nu_{in})\right]^{1/2}/\hat{k}\hat{d} \tag{41}$$

The negative (positive) sign on the right hand side yields a growing (damped) mode. In the following anlaysis we consider the growing modes.

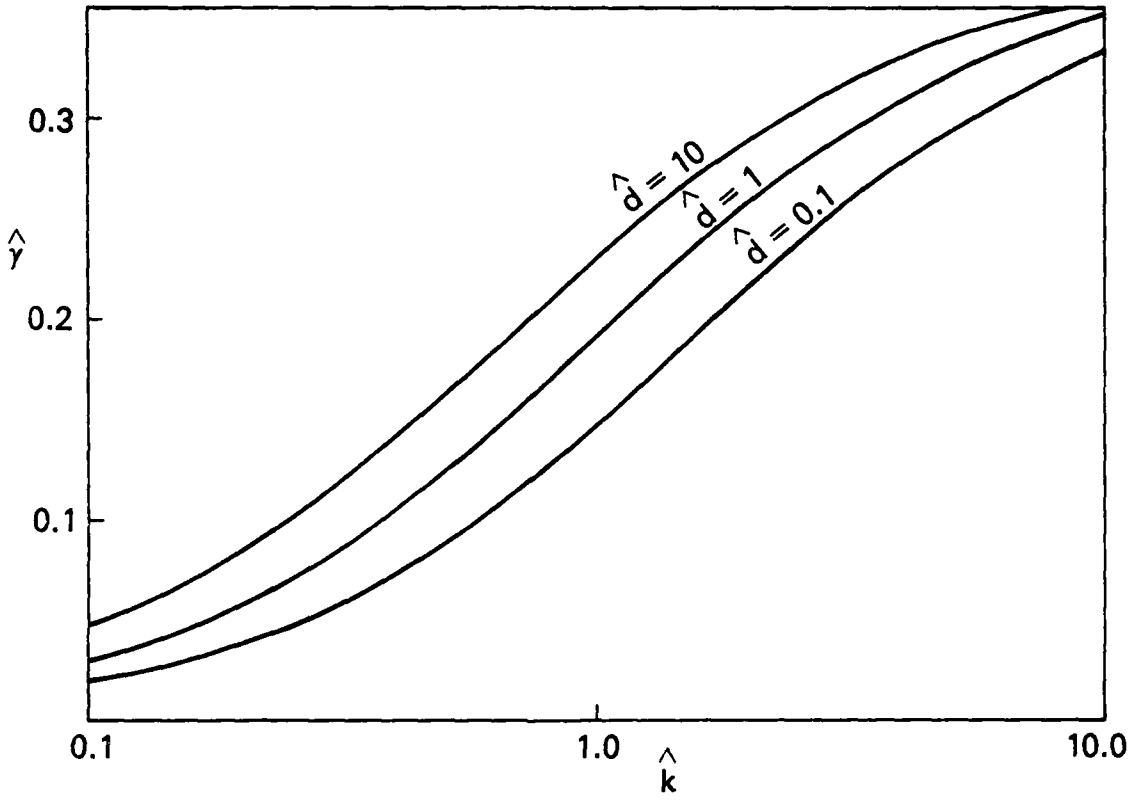

Figure 5

Plot of growth rate $\hat{\gamma}$ versus $\hat{d}$ for $\hat{k} = 0.5$, 1.0, 10.0 and 100.0, and for the same parameters as in Fig. 3. Note that $\hat{\gamma} \to \hat{\gamma}_L$ (Eq. 38) for $\hat{d} \to \infty$.

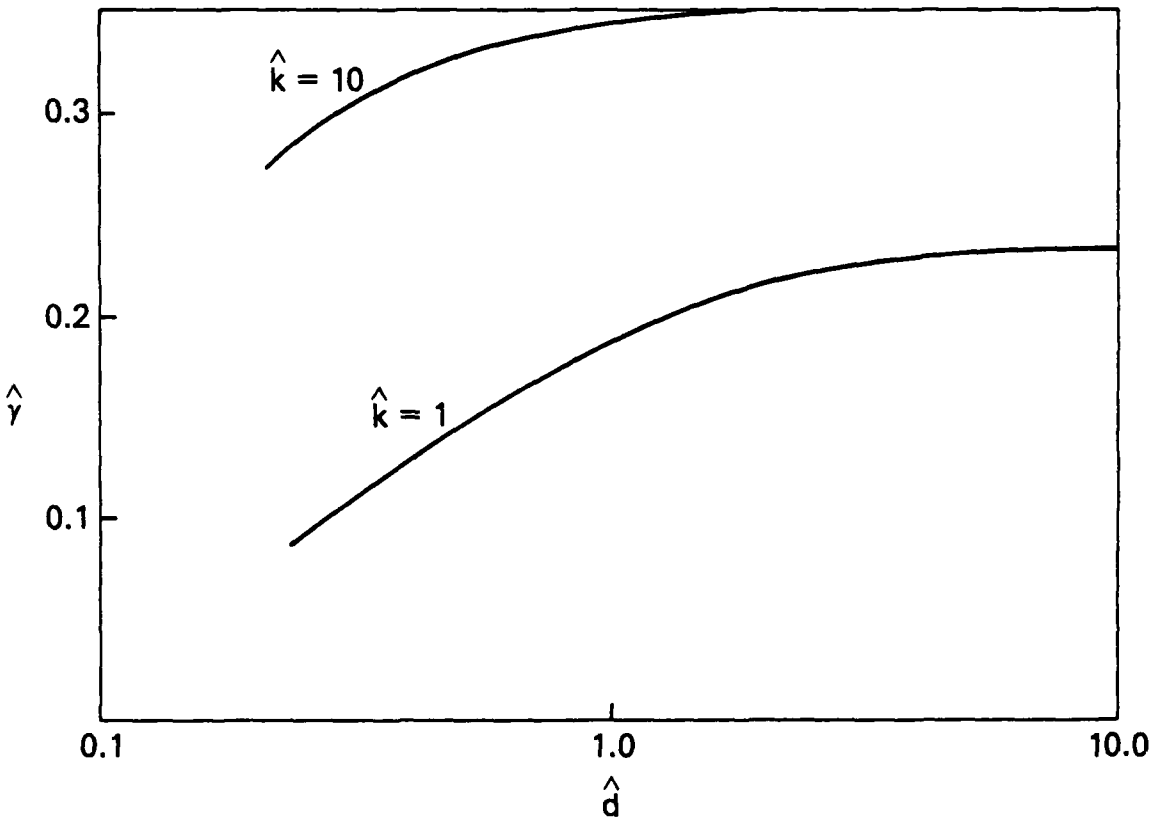

Figure 6

Plot of growth rate $\hat{\gamma}$ versus finite current channel width $\hat{d}$ for diffuse boundary case and for the same parameters as in Fig. 3.

REFERENCES

Bakshi, P., G. Ganguli, and P. Palmadesso, Finite width currents, magnetic shear, and the current-driven ion-cyclotron instability, Phys. Fluids, 26, 1808, 1983.

Bythrow, P.F., T.A. Potemra, L.J. Zanetti, C. Meng, R.E. Huffman, F.J. Rich, D.A. Hardy, W.B. Hanson, R.A. Heelis, Earthward directed high density Birkeland currents observed by HILAT, J. Geophys. Res. (in press, 1984).

Chaturvedi, P.K., and S.L. Ossakow, Nonlinear stabilization of the current convective instability in the diffuse aurora, Geophys. Res. Lett., 6, 957, 1979.

Chaturvedi, P.K., and S.L. Ossakow, The current convective instability as applied to the auroral ionosphere, J. Geophys. Res., 86, 4811, 1981.

Chaturvedi, P.K., and S.L. Ossakow, Effect of an electron beam on the current convective instability, J. Geophys. Res., 88, 4119, 1983.

Chen, J., and P. Palmadesso, Tearing instability in an anisotropic neutral sheet, Phys. Fluids, 27, 1198, 1984.

Fejer, B.G., and M.C. Kelley, Ionospheric Irregularities, Rev. Geophys. and Space Phys., 18, 401, 1980.

Ganguli, G., P. Bakshi, and P. Palmadesso, Electrostatic ion-cyclotron waves in magnetospheric plasmas: Nonlocal aspects, J. Geophys. Res., 89, 945, 1984.

Gary, S.P., Kinetic theory of current and density drift instabilities with weak charged-neutral collisions, J. Geophys. Res., 89, 179, 1984.

Hanuise, C., J.P. Villain, and M. Crochet, Spectral studies of F region irregularities in the auroral zone, Geophys. Res. Lett., 8, 1083, 1981.

Huba, J.D., and S.L. Ossakow, Influence of magnetic shear on the current convective instability in the diffuse aurora, J. Geophys. Res., 85, 6874, 1980.

Huba, J.D., Long wavelength limit of the current convective instability, J. Geophys. Res., 89, 2931, 1984.

Huba, J.D., S.L. Ossakow, P.Satyanarayana, and P. N. Guzdar, Linear theory of the $\underline{E} \times \underline{B}$ instability with an inhomogeneous electric field, J. Geophy. Res., 88, 425, 1983.

Kadomtsev, B.B. and A.V. Nedospasov, Instability of the positive column in a magnetic field and the "anomalous diffusion effect," J. Nucl. Energy, Part C, 1, 230, 1960.

Keskinen, M.J., S.L. Ossakow, and B.E. McDonald, Nonlinear evolution of diffuse auroral F region ionospheric irregularities, Geophys. Res. Lett., 7, 573, 1980.

Keskinen, M.J., and S.L. Ossakow, Nonlinear evolution of plasma enhancements in the auroral ionosphere 1. long wavelength irregularities, J. Geophys. Res., 87, 144, 1982.

Keskinen, M.J., and S.L. Ossakow, Nonlinear evolution of convecting plasma enhancements in the auroral ionosphere 2. small scale irregularities, J. Geophys. Res., 88, 474, 1983.

Keskinen, M.J. and S.L. Ossakow, Theories of high-latitude ionospheric irreguarities: A review, Radio Sci., 18, 1077, 1983.

Keskinen, M.J., Nonlinear theory of the E x B instability with an inhomogeneous electric field, J. Geophys. Res., 89, 3913, 1984.

Lehnert, B., Diffusion processes in the positive column in a longitudinal magnetic field, in Proceedings of the Second Geneva Conference on the Peaceful Uses of Atomic Energy, 32, 349, 1958.

Linson, L.M., and J.B. Workman, Formation of striations in ionospheric plasma clouds, J. Geophys. Res., 75, 3211, 1970.

Ossakow, S.L. and P.K. Chaturvedi, Current convective instability in the diffuse aurora, Geophys. Res. Lett., 6, 332, 1979.

Satyanarayana, P., and S.L. Ossakow, Velocity shear stabilization of the current convective instability, J. Geophys. Res., 89, 3019, 1984.

Simon, A., Instability of a partially ionized plasma in crossed electric and magnetic fields, Phys. Fluids, 6, 382, 1963.

Vickrey, J.F., C.L. Rino, and T.A. Potemra, Chatanika/Triad observations of unstable ionization enhancements in the auroral F-region, Geophys. Res. Lett., 7, 789, 1980.

Vickrey, J.F., and M.C. Kelley, Irregularities and instabilities in the auroral F-region, High Latitude Space Plasma Physics, ed. B. Hultquist and T. Hagfors, Plenum, New York, 1983.

DISTRIBUTION LIST

DEPARTMENT OF DEFENSE

ASSISTANT SECRETARY OF DEFENSE
COMM, CMD, CONT 7 INTELL
WASHINGTON, D.C. 20301

DIRECTOR
COMMAND CONTROL TECHNICAL CENTER
PENTAGON RM BE 685
WASHINGTON, D.C. 20301
01CY ATTN C-650
01CY ATTN C-312 R. MASON

DIRECTOR
DEFENSE ADVANCED RSCH PROJ AGENCY
ARCHITECT BUILDING
1400 WILSON BLVD.
ARLINGTON, VA. 22209
01CY ATTN NUCLEAR MONITORING RESEARCH
01CY ATTN STRATEGIC TECH OFFICE

DEFENSE COMMUNICATION ENGINEER CENTER
1860 WIEHLE AVENUE
RESTON, VA. 22090
01CY ATTN CODE R410
01CY ATTN CODE R812

DEFENSE TECHNICAL INFORMATION CENTER
CAMERON STATION
ALEXANDRIA, VA. 22314
02CY

DIRECTOR
DEFENSE NUCLEAR AGENCY
WASHINGTON, D.C. 20305
01CY ATTN STVL
04CY ATTN TITL
01CY ATTN DDST
03CY ATTN RAAE

COMMANDER
FIELD COMMAND
DEFENSE NUCLEAR AGENCY
KIRTLAND, AFB, NM 87115
01CY ATTN FCPR

DEFENSE NUCLEAR AGENCY
SAO/DNA
BUILDING 20676
KIRTLAND AFB, NM 87115
01CY D.C. THORNBURG

DIRECTOR
INTERSERVICE NUCLEAR WEAPONS SCHOOL
KIRTLAND AFB, NM 87115
01CY ATTN DOCUMENT CONTROL

JOINT CHIEFS OF STAFF
WASHINGTON, D.C. 20301
01CY ATTN J-3 WWMCCS EVALUATION OFFICE

DIRECTOR
JOINT STRAT TGT PLANNING STAFF
OFFUTT AFB
OMAHA, NB 68113
01CY ATTN JSTPS/JLKS
01CY ATTN JPST G. GOETZ

CHIEF
LIVERMORE DIVISION FLD COMMAND DNA
DEPARTMENT OF DEFENSE
LAWRENCE LIVERMORE LABORATORY
P.O. BOX 808
LIVERMORE, CA 94550
01CY ATTN FCPRL

COMMANDANT
NATO SCHOOL (SHAPE)
APO NEW YORK 09172
01CY ATTN U.S. DOCUMENTS OFFICER

UNDER SECY OF DEF FOR RSCH & ENGRG
DEPARTMENT OF DEFENSE
WASHINGTON, D.C. 20301
01CY ATTN STRATEGIC & SPACE SYSTEMS (OS)

WWMCCS SYSTEM ENGINEERING ORG
WASHINGTON, D.C. 20305
01CY ATTN R. CRAWFORD

COMMANDER/DIRECTOR
ATMOSPHERIC SCIENCES LABORATORY
U.S. ARMY ELECTRONICS COMMAND
WHITE SANDS MISSILE RANGE, NM 88002
01CY ATTN DELAS-EO, F. NILES

DIRECTOR
BMD ADVANCED TECH CTR
HUNTSVILLE OFFICE
P.O. BOX 1500
HUNTSVILLE, AL 35807
01CY ATTN ATC-T MELVIN T. CAPPS
01CY ATTN ATC-O W. DAVIES
01CY ATTN ATC-R DON RUSS

PROGRAM MANAGER
BMD PROGRAM OFFICE
5001 EISENHOWER AVENUE
ALEXANDRIA, VA 22333
01CY ATTN DACS-BMT J. SHEA

CHIEF C-E- SERVICES DIVISION
U.S. ARMY COMMUNICATIONS CMD
PENTAGON RM 1B269
WASHINGTON, D.C. 20310
01CY ATTN C- E-SERVICES DIVISION

COMMANDER
FRADCOM TECHNICAL SUPPORT ACTIVITY
DEPARTMENT OF THE ARMY
FORT MONMOUTH, N.J. 07703
01CY ATTN DRSEL-NL-RD H. BENNET
01CY ATTN DRSEL-PL-ENV H. BOMKE
01CY ATTN J.E. QUIGLEY

COMMANDER
U.S. ARMY COMM-ELEC ENGRG INSTAL AGY
FT. HUACHUCA, AZ 85613
01CY ATTN CCC-EMEO GEORGE LANE

COMMANDER
U.S. ARMY FOREIGN SCIENCE & TECH CTR
220 7TH STREET, NE
CHARLOTTESVILLE, VA 22901
01CY ATTN DRXST-SD

COMMANDER
U.S. ARMY MATERIAL DEV & READINESS CMD
5001 EISENHOWER AVENUE
ALEXANDRIA, VA 22333
01CY ATTN DRCLDC J.A. BENDER

COMMANDER
U.S. ARMY NUCLEAR AND CHEMICAL AGENCY
7500 BACKLICK ROAD
BLDG 2073
SPRINGFIELD, VA 22150
01CY ATTN LIBRARY

DIRECTOR
U.S. ARMY BALLISTIC RESEARCH
LABORATORY
ABERDEEN PROVING GROUND, MD 21005
01CY ATTN TECH LIBRARY,
EDWARD BAICY

COMMANDER
U.S. ARMY SATCOM AGENCY
FT. MONMOUTH, NJ 07703
01CY ATTN DOCUMENT CONTROL

COMMANDER
U.S. ARMY MISSILE INTELLIGENCE AGENCY
REDSTONE ARSENAL, AL 35809
01CY ATTN JIM GAMBLE

DIRECTOR
U.S. ARMY TRADOC SYSTEMS ANALYSIS
ACTIVITY
WHITE SANDS MISSILE RANGE, NM 88002
01CY ATTN ATAA-SA
01CY ATTN TCC/F. PAYAN JR.
01CY ATTN ATTA-TAC LTC J. HESSE

COMMANDER
NAVAL ELECTRONIC SYSTEMS COMMAND
WASHINGTON, D.C. 20360
01CY ATTN NAVALEX 034 T. HUGHES
01CY ATTN PME 117
01CY ATTN PME 117-T
01CY ATTN CODE 5011

COMMANDING OFFICER
NAVAL INTELLIGENCE SUPPORT CTR
4301 SUITLAND ROAD, BLDG. 5
WASHINGTON, D.C. 20390
01CY ATTN MR. DUBBIN STIC 12
01CY ATTN NISC-50
01CY ATTN CODE 5404 J. GALET

COMMANDER
NAVAL OCCEAN SYSTEMS CENTER
SAN DIEGO, CA 92152
01CY ATTN J. FERGUSON

NAVAL RESEARCH LABORATORY
WASHINGTON, D.C. 20375
01CY ATTN CODE 4700 S. L. Ossakow
26 CYS IF UNCLASS, 1 CY
IF CLASS)
01CY ATTN CODE 4701 I Vitkovitsky
01CY ATTN CODE 4780 J. Huba (100
CYS IF UNCLASS, 1 CY IF CLASS)
01CY ATTN CODE 7500
01CY ATTN CODE 7550
01CY ATTN CODE 7580
01CY ATTN CODE 7551
01CY ATTN CODE 7555
01CY ATTN CODE 4730 E. MCLEAN
01CY ATTN CODE 4108
01CY ATTN CODE 4730 B. RIPIN
20CY ATTN CODE 2628

COMMANDER
NAVAL SPACE SURVEILLANCE SYSTEM
DAHLGREN, VA 22448
01CY ATTN CAPT J.H. BURTON

OFFICER-IN-CHARGE
NAVAL SURFACE WEAPONS CENTER
WHITE OAK, SILVER SPRING, MD 20910
01CY ATTN CODE F31

DIRECTOR
STRATEGIC SYSTEMS PROJECT OFFICE
DEPARTMENT OF THE NAVY
WASHINGTON, D.C. 20376
01CY ATTN NSP-2141
01CY ATTN NSSP-2722 FRED WIMBERLY

COMMANDER
NAVAL SURFACE WEAPONS CENTER
DAHLGREN LABORATORY
DAHLGREN, VA 22448
01CY ATTN CODE DF-14 R. BUTLER

OFFICER OF NAVAL RESEARCH
ARLINGTON, VA 22217
01CY ATTN CODE 465
01CY ATTN CODE 461
01CY ATTN CODE 402
01CY ATTN CODE 420
01CY ATTN CODE 421

COMMANDER
AEROSPACE DEFENSE COMMAND/DC
DEPARTMENT OF THE AIR FORCE
ENT AFB, CO 80912
01CY ATTN DC MR. LONG

COMMANDER
AEROSPACE DEFENSE COMMAND/XPD
DEPARTMENT OF THE AIR FORCE
ENT AFB, CO 80912
01CY ATTN XPDQQ
01CY ATTN XP

AIR FORCE GEOPHYSICS LABORATORY
HANSCOM AFB, MA 01731
01CY ATTN OPR HAROLD GARDNER
01CY ATTN LKB
KENNETH S.W. CHAMPION
01CY ATTN OPR ALVA T. STAIR
01CY ATTN PHD JURGEN BUCHAU
01CY ATTN PHD JOHN P. MULLEN

AF WEAPONS LABORATORY
KIRTLAND AFT, NM 87117
01CY ATTN SUL
01CY ATTN CA ARTHUR H. GUENTHER
01CY ATTN NTYCE 1LT. G. KRAJEI

AFTAC
PATRICK AFB, FL 32925
01CY ATTN TN

AIR FORCE AVIONICS LABORATORY
WRIGHT-PATTERSON AFB, OH 45433
01CY ATTN AAD WADE HUNT
01CY ATTN AAD ALLEN JOHNSON

DEPUTY CHIEF OF STAFF
RESEARCH, DEVELOPMENT, & ACQ
DEPARTMENT OF THE AIR FORCE
WASHINGTON, D.C. 20330
01CY ATTN AFRDQ

HEADQUARTERS
ELECTRONIC SYSTEMS DIVISION
DEPARTMENT OF THE AIR FORCE
HANSCOM AFB, MA 01731
01CY ATTN J. DEAS

HEADQUARTERS
ELECTRONIC SYSTEMS DIVISION/YSEA
DEPARTMENT OF THE AIR FORCE
HANSCOM AFB, MA 01732
01CY ATTN YSEA

HEADQUARTERS
ELECTRONIC SYSTEMS DIVISION/DC
DEPARTMENT OF THE AIR FORCE
HANSCOM AFB, MA 01731
01CY ATTN DCKC MAJ J.C. CLARK

COMMANDER
FOREIGN TECHNOLOGY DIVISION, AFSC
WRIGHT-PATTERSON AFB, OH 45433
01CY ATTN NICD LIBRARY
01CY ATTN ETDP B. BALLARD

COMMANDER
ROME AIR DEVELOPMENT CENTER, AFSC
GRIFFISS AFB, NY 13441
01CY ATTN DOC LIBRARY/TSLD
01CY ATTN OCSE V. COYNE

SAMSO/SZ
POST OFFICE BOX 92960
WORLDWAY POSTAL CENTER
LOS ANGELES, CA 90009
(SPACE DEFENSE SYSTEMS)
01CY ATTN SZJ

STRATEGIC AIR COMMAND/XPFS
OFFUTT AFB, NB 68113
01CY ATTN ADWATE MAJ BRUCE BAUER
01CY ATTN NRT
01CY ATTN DOK CHIEF SCIENTIST

SAMSO/SK
P.O. BOX 92960
WORLDWAY POSTAL CENTER
LOS ANGELES, CA 90009
01CY ATTN SKA (SPACE COMM SYSTEMS)
M. CLAVIN

SAMSO/MN
NORTON AFB, CA 92409
(MINUTEMAN)
01CY ATTN MNNL

COMMANDER
ROME AIR DEVELOPMENT CENTER, AFSC
HANSCOM AFB, MA 01731
01CY ATTN EEP A. LORENTZEN

DEPARTMENT OF ENERGY
LIBRARY ROOM G-042
WASHINGTON, D.C. 20545
01CY ATTN DOC CON FOR A. LABOWITZ

DEPARTMENT OF ENERGY
ALBUQUERQUE OPERATIONS OFFICE
P.O. BOX 5400
ALBUQUERQUE, NM 87115
01CY ATTN DOC CON FOR D. SHERWOOD

EG&G, INC.
LOS ALAMOS DIVISION
P.O. BOX 809
LOS ALAMOS, NM 85544
01CY ATTN DOC CON FOR J. BREEDLOVE

UNIVERSITY OF CALIFORNIA
LAWRENCE LIVERMORE LABORATORY
P.O. BOX 808
LIVERMORE, CA 94550
01CY ATTN DOC CON FOR TECH INFO
DEPT
01CY ATTN DOC CON FOR L-389 R. OTT
01CY ATTN DOC CON FOR L-31 R. HAGER

LOS ALAMOS NATIONAL LABORATORY
P.O. BOX 1663
LOS ALAMOS, NM 87545
01CY ATTN DOC CON FOR J. WOLCOTT
01CY ATTN DOC CON FOR R.F. TASCHEK
01CY ATTN DOC CON FOR E. JONES
01CY ATTN DOC CON FOR J. MALIK
01CY ATTN DOC CON FOR R. JEFFRIES
01CY ATTN DOC CON FOR J. ZINN
01CY ATTN DOC CON FOR P. KEATON
01CY ATTN DOC CON FOR D. WESTERVELT
01CY ATTN D. SAPPENFIELD

SANDIA LABORATORIES
P.O. BOX 5800
ALBUQUERQUE, NM 87115
01CY ATTN DOC CON FOR W. BROWN
01CY ATTN DOC CON FOR A.
THORNBROUGH
01CY ATTN DOC CON FOR T. WRIGHT
01CY ATTN DOC CON FOR D. DAHLGREN
01CY ATTN DOC CON FOR 3141
01CY ATTN DOC CON FOR SPACE PROJECT
DIV

SANDIA LABORATORIES
LIVERMORE LABORATORY
P.O. BOX 969
LIVERMORE, CA 94550
01CY ATTN DOC CON FOR B. MURPHEY
01CY ATTN DOC CON FOR T. COOK

OFFICE OF MILITARY APPLICATION
DEPARTMENT OF ENERGY
WASHINGTON, D.C. 20545
01CY ATTN DOC CON DR. YO SONG

OTHER GOVERNMENT

INSTITUTE FOR TELECOM SCIENCES
NATIONAL TELECOMMUNICATIONS & INFO ADMIN
BOULDER, CO 80303
01CY ATTN A. JEAN (UNCLASS ONLY)
01CY ATTN W. UTLAUT
01CY ATTN D. CROMBIE
01CY ATTN L. BERRY

NATIONAL OCEANIC & ATMOSPHERIC ADMIN
ENVIRONMENTAL RESEARCH LABORATORIES
DEPARTMENT OF COMMERCE
BOULDER, CO 80302
01CY ATTN R. GRUBB
01CY ATTN AERONOMY LAB G. REID

DEPARTMENT OF DEFENSE CONTRACTORS

AEROSPACE CORPORATION
P.O. BOX 92957
LOS ANGELES, CA 90009
01CY ATTN I. GARFUNKEL
01CY ATTN T. SALMI
01CY ATTN V. JOSEPHSON
01CY ATTN S. BOWER
01CY ATTN D. OLSEN

ANALYTICAL SYSTEMS ENGINEERING CORP
5 OLD CONCORD ROAD
BURLINGTON, MA 01803
01CY ATTN RADIO SCIENCES

AUSTIN RESEARCH ASSOC., INC.
1901 RUTLAND DRIVE
AUSTIN, TX 78758
01CY ATTN L. SLOAN
01CY ATTN R. THOMPSON

BERKELEY RESEARCH ASSOCIATES, INC.
P.O. BOX 983
BERKELEY, CA 94701
01CY ATTN J. WORKMAN
01CY ATTN C. PRETTIE
01CY ATTN S. BRECHT

BOEING COMPANY, THE
P.O. BOX 3707
SEATTLE, WA 98124
01CY ATTN G. KEISTER
01CY ATTN D. MURRAY
01CY ATTN G. HALL
01CY ATTN J. KENNEY

CHARLES STARK DRAPER LABORATORY, INC.
555 TECHNOLOGY SQUARE
CAMBRIDGE, MA 02139
01CY ATTN D.B. COX
01CY ATTN J.P. GILMORE

COMSAT LABORATORIES
LINTHICUM ROAD
CLARKSBURG, MD 20734
01CY ATTN G. HYDE

CORNELL UNIVERSITY
DEPARTMENT OF ELECTRICAL ENGINEERING
ITHACA, NY 14850
01CY ATTN D.T. FARLEY, JR.

ELECTROSPACE SYSTEMS, INC.
BOX 1359
RICHARDSON, TX 75080
01CY ATTN H. LOGSTON
01CY ATTN SECURITY (PAUL PHILLIPS)

EOS TECHNOLOGIES, INC.
606 Wilshire Blvd.
Santa Monica, Calif 90401
01CY ATTN C.B. GABBARD
01CY ATTN R. LELEVIER

ESL, INC.
495 JAVA DRIVE
SUNNYVALE, CA 94086
01CY ATTN J. ROBERTS
01CY ATTN JAMES MARSHALL

GENERAL ELECTRIC COMPANY
SPACE DIVISION
VALLEY FORGE SPACE CENTER
GODDARD BLVD KING OF PRUSSIA
P.O. BOX 8555
PHILADELPHIA, PA 19101
01CY ATTN M.H. BORTNER
SPACE SCI LAB

GENERAL ELECTRIC COMPANY
P.O. BOX 1122
SYRACUSE, NY 13201
01CY ATTN F. REIBERT

GENERAL ELECTRIC TECH SERVICES CO., INC.
HMES
COURT STREET
SYRACUSE, NY 13201
01CY ATTN G. MILLMAN

GEOPHYSICAL INSTITUTE
UNIVERSITY OF ALASKA
FAIRBANKS, AK 99701
(ALL CLASS ATTN: SECURITY OFFICER)
01CY ATTN T.N. DAVIS (UNCLASS ONLY)
01CY ATTN TECHNICAL LIBRARY
01CY ATTN NEAL BROWN (UNCLASS ONLY)

GTE SYLVANIA, INC.
ELECTRONICS SYSTEMS GRP-EASTERN DIV
77 A STREET
NEEDHAM, MA 02194
01CY ATTN DICK STEINHOF

HSS, INC.
2 ALFRED CIRCLE
BEDFORD, MA 01730
01CY ATTN DONALD HANSEN

ILLINOIS, UNIVERSITY OF
107 COBLE HALL
150 DAVENPORT HOUSE
CHAMPAIGN, IL 61820
(ALL CORRES ATTN DAN MCCLELLAND)
01CY ATTN K. YEH

INSTITUTE FOR DEFENSE ANALYSES
1801 NO. BEAUREGARD STREET
ALEXANDRIA, VA 22311
01CY ATTN J.M. AEIN
01CY ATTN ERNEST BAUER
01CY ATTN HANS WOLFARD
01CY ATTN JOEL BENGSTON

INTL TEL & TELEGRAPH CORPORATION
500 WASHINGTON AVENUE
NUTLEY, NJ 07110
01CY ATTN TECHNICAL LIBRARY

JAYCOR
11011 TORREYANA ROAD
P.O. BOX 85154
SAN DIEGO, CA 92138
01CY ATTN J.L. SPERLING

JOHNS HOPKINS UNIVERSITY
APPLIED PHYSICS LABORATORY
JOHNS HOPKINS ROAD
LAUREL, MD 20810
01CY ATTN DOCUMENT LIBRARIAN
01CY ATTN THOMAS POTEMRA
01CY ATTN JOHN DASSOULAS

KAMAN SCIENCES CORP
P.O. BOX 7463
COLORADO SPRINGS, CO 80933
01CY ATTN T. MEAGHER

KAMAN TEMPO-CENTER FOR ADVANCED STUDIES
816 STATE STREET (P.O DRAWER QQ)
SANTA BARBARA, CA 93102
01CY ATTN DASIAC
01CY ATTN WARREN S. KNAPP
01CY ATTN WILLIAM MCNAMARA
01CY ATTN B. GAMBILL

LINKABIT CORP
10453 ROSELLE
SAN DIEGO, CA 92121
01CY ATTN IRWIN JACOBS

LOCKHEED MISSILES & SPACE CO., INC
P.O. BOX 504
SUNNYVALE, CA 94088
01CY ATTN DEPT 60-12
01CY ATTN D.R. CHURCHILL

LOCKHEED MISSILES & SPACE CO., INC.
3251 HANOVER STREET
PALO ALTO, CA 94304
01CY ATTN MARTIN WALT DEPT 52-12
01CY ATTN W.L. IMHOF DEPT 52-12
01CY ATTN RICHARD G. JOHNSON DEPT 52-12
01CY ATTN J.B. CLADIS DEPT 52-12

MARTIN MARIETTA CORP
ORLANDO DIVISION
P.O. BOX 5837
ORLANDO, FL 32805
01CY ATTN R. HEFFNER

M.I.T. LINCOLN LABORATORY
P.O. BOX 73
LEXINGTON, MA 02173
01CY ATTN DAVID M. TOWLE
01CY ATTN L. LOUGHLIN
01CY ATTN D. CLARK

MCDONNEL DOUGLAS CORPORATION
5301 BOLSA AVENUE
HUNTINGTON BEACH, CA 92647
01CY ATTN N. HARRIS
01CY ATTN J. MOULE
01CY ATTN GEORGE MROZ
01CY ATTN W. OLSON
01CY ATTN R.W. HALPRIN
01CY ATTN TECHNICAL LIBRARY SERVICES

MISSION RESEARCH CORPORATION
735 STATE STREET
SANTA BARBARA, CA 93101
01CY ATTN P. FISCHER
01CY ATTN W.F. CREVIER
01CY ATTN STEVEN L. GUTSCHE
01CY ATTN R. BOGUSCH
01CY ATTN R. HENDRICK
01CY ATTN RALPH KILB
01CY ATTN DAVE SOWLE
01CY ATTN F. FAJEN
01CY ATTN M. SCHEIBE
01CY ATTN CONRAD L. LONGMIRE
01CY ATTN B. WHITE
01CY ATTN R. STAGAT

MISSION RESEARCH CORP.
1720 RANDOLPH ROAD, S.E.
ALBUQUERQUE, NEW MEXICO 87106
01CY R. STELLINGWERF
01CY M. ALME
01CY L. WRIGHT

MITRE CORPORATION, THE
P.O. BOX 208
BEDFORD, MA 01730
01CY ATTN JOHN MORGANSTERN
01CY ATTN G. HARDING
01CY ATTN C.E. CALLAHAN

MITRE CORP
WESTGATE RESEARCH PARK
1820 DOLLY MADISON BLVD
MCLEAN, VA 22101
01CY ATTN W. HALL
01CY ATTN W. FOSTER

PACIFIC-SIERRA RESEARCH CORP
12340 SANTA MONICA BLVD.
LOS ANGELES, CA 90025
01CY ATTN E.C. FIELD, JR.

PENNSYLVANIA STATE UNIVERSITY
IONOSPHERE RESEARCH LAB
318 ELECTRICAL ENGINEERING EAST
UNIVERSITY PARK, PA 16802
(NO CLASS TO THIS ADDRESS)
01CY ATTN IONOSPHERIC RESEARCH LAB

PHOTOMETRICS, INC.
4 ARROW DRIVE
WOBURN, MA 01801
01CY ATTN IRVING L. KOFSKY

PHYSICAL DYNAMICS, INC.
P.O. BOX 3027
BELLEVUE, WA 98009
01CY ATTN E.J. FREMOUW

PHYSICAL DYNAMICS, INC.
P.O. BOX 10367
OAKLAND, CA 94610
ATTN A. THOMSON

R & D ASSOCIATES
P.O. BOX 9695
MARINA DEL REY, CA 90291
01CY ATTN FORREST GILMORE
01CY ATTN WILLIAM B. WRIGHT, JR.
01CY ATTN WILLIAM J. KARZAS
01CY ATTN H. ORY
01CY ATTN C. MACDONALD
01CY ATTN R. TURCO
01CY ATTN L. DeRAND
01CY ATTN W. TSAI

RAND CORPORATION, THE
1700 MAIN STREET
SANTA MONICA, CA 90406
01CY ATTN CULLEN CRAIN
01CY ATTN ED BEDROZIAN

RAYTHEON CO.
528 BOSTON POST ROAD
SUDBURY, MA 01776
01CY ATTN BARBARA ADAMS

RIVERSIDE RESEARCH INSTITUTE
330 WEST 42nd STREET
NEW YORK, NY 10036
01CY ATTN VINCE TRAPANI

SCIENCE APPLICATIONS, INC.
1150 PROSPECT PLAZA
LA JOLLA, CA 92037
01CY ATTN LEWIS M. LINSON
01CY ATTN DANIEL A. HAMLIN
01CY ATTN E. FRIEMAN
01CY ATTN E.A. STRAKER
01CY ATTN CURTIS A. SMITH

SCIENCE APPLICATIONS, INC
1710 GOODRIDGE DR.
MCLEAN, VA 22102
01CY J. COCKAYNE
01CY E. HYMAN

SRI INTERNATIONAL
333 RAVENSWOOD AVENUE
MENLO PARK, CA 94025
01CY ATTN J. CASPER
01CY ATTN DONALD NEILSON
01CY ATTN ALAN BURNS
01CY ATTN G. SMITH
01CY ATTN R. TSUNODA
01CY ATTN DAVID A. JOHNSON
01CY ATTN WALTER G. CHESNUT
01CY ATTN CHARLES L. RINO
01CY ATTN WALTER JAYE
01CY ATTN J. VICKREY
01CY ATTN RAY L. LEADABRAND
01CY ATTN G. CARPENTER
01CY ATTN G. PRICE
01CY ATTN R. LIVINGSTON
01CY ATTN V. GONZALES
01CY ATTN D. MCDANIEL

TECHNOLOGY INTERNATIONAL CORP
75 WIGGINS AVENUE
BEDFORD, MA 01730
01CY ATTN W.P. BOQUIST

TOYON RESEARCH CO.
P.O. Box 6890
SANTA BARBARA, CA 93111
01CY ATTN JOHN ISE, JR.
01CY ATTN JOEL GARBARINO

TRW DEFENSE & SPACE SYS GROUP
ONE SPACE PARK
REDONDO BEACH, CA 90278
01CY ATTN R. K. PLEBUCH
01CY ATTN S. ALTSCHULER
01CY ATTN D. DEE
01CY ATTN D/ STOCKWELL
SNTF/1575

VISIDYNE
SOUTH BEDFORD STREET
BURLINGTON, MASS 01803
01CY ATTN W. REIDY
01CY ATTN J. CARPENTER
01CY ATTN C. HUMPHREY

UNIVERSITY OF PITTSBURGH
PITTSBURGH, PA 15213
01CY ATTN: N. ZABUSKY

IONOSPHERIC MODELING DISTRIBUTION LIST
(UNCLASSIFIED ONLY)

PLEASE DISTRIBUTE ONE COPY TO EACH OF THE FOLLOWING PEOPLE (UNLESS OTHERWISE NOTED)

NAVAL RESEARCH LABORATORY
WASHINGTON, D.C. 20375
Code 4100
Dr. H. GURSKY - CODE 4100
Dr. P. GOODMAN - CODE 4180

A.F. GEOPHYSICS LABORATORY
L.G. HANSCOM FIELD
BEDFORD, MA 01731
DR. T. ELKINS
DR. W. SWIDER
MRS. R. SAGALYN
DR. J.M. FORBES
DR. T.J. KENESHEA
DR. W. BURKE
DR. H. CARLSON
DR. J. JASPERS
Dr. F.J. RICH
DR. N. MAYNARD

BOSTON UNIVERSITY
DEPARTMENT OF ASTRONOMY
BOSTON, MA 02215
DR. J. AARONS

CORNELL UNIVERSITY
ITHACA, NY 14850
DR. W.E. SWARTZ
DR. D. FARLEY
DR. M. KELLEY

HARVARD UNIVERSITY
HARVARD SQUARE
CAMBRIDGE, MA 02138
DR. M.B. McELROY
DR. R. LINDZEN

INSTITUTE FOR DEFENSE ANALYSIS
400 ARMY/NAVY DRIVE
ARLINGTON, VA 22202
DR. E. BAUER

MASSACHUSETTS INSTITUTE OF TECHNOLOGY
PLASMA FUSION CENTER
LIBRARY, NW16-262
CAMBRIDGE, MA 02139

NASA
GODDARD SPACE FLIGHT CENTER
GREENBELT, MD 20771
DR. K. MAEDA
DR. S. CURTIS
DR. M. DUBIN

COMMANDER
NAVAL AIR SYSTEMS COMMAND
DEPARTMENT OF THE NAVY
WASHINGTON, D.C. 20360
DR. T. CZUBA

COMMANDER
NAVAL OCEAN SYSTEMS CENTER
SAN DIEGO, CA 92152
MR. R. ROSE - CODE 5321

NOAA
DIRECTOR OF SPACE AND ENVIRONMENTAL LABORATORY
BOULDER, CO 80302
DR. A. GLENN JEAN
DR. G.W. ADAMS
DR. D.N. ANDERSON
DR. K. DAVIES
DR. R.F. DONNELLY

OFFICE OF NAVAL RESEARCH
800 NORTH QUINCY STREET
ARLINGTON, VA 22217
DR. G. JOINER

PENNSYLVANIA STATE UNIVERSITY
UNIVERSITY PARK, PA 16802
DR. J.S. NISBET
DR. P.R. ROHRBAUGH
DR. L.A. CARPENTER
DR. M. LEE
DR. R. DIVANY
DR. P. BENNETT
DR. F. KLEVANS

SCIENCE APPLICATIONS, INC.
1150 PROSPECT PLAZA
LA JOLLA, CA 92037
DR. D.A. HAMLIN
DR. E. FRIEMAN

STANFORD UNIVERSITY
STANFORD, CA 94305
DR. P.M. BANKS

U.S. ARMY ABERDEEN RESEARCH
AND DEVELOPMENT CENTER
BALLISTIC RESEARCH LABORATORY
ABERDEEN, MD
DR. J. HEIMERL

GEOPHYSICAL INSTITUTE
UNIVERSITY OF ALASKA
FAIRBANKS, AK 99701
DR. L.E. LEE

UNIVERSITY OF CALIFORNIA,
BERKELEY
BERKELEY, CA 94720
DR. M. HUDSON

UNIVERSITY OF CALIFORNIA
LOS ALAMOS SCIENTIFIC LABORATORY
J-10, MS-664
LOS ALAMOS, NM 87545
DR. M. PONGRATZ
DR. D. SIMONS
DR. G. BARASCH
DR. L. DUNCAN
DR. P. BERNHARDT
DR. S.P. GARY

UNIVERSITY OF MARYLAND
COLLEGE PARK, MD 20740
DR. K. PAPADOPOULOS
DR. E. OTT

JOHNS HOPKINS UNIVERSITY
APPLIED PHYSICS LABORATORY
JOHNS HOPKINS ROAD
LAUREL, MD 20810
DR. R. GREENWALD
DR. C. MENG

UNIVERSITY OF PITTSBURGH
PITTSBURGH, PA 15213
DR. N. ZABUSKY
DR. M. BIONDI
DR. E. OVERMAN

UNIVERSITY OF TEXAS
AT DALLAS
CENTER FOR RESEARCH SCIENCES
P.O. BOX 688
RICHARDSON, TX 75080
DR. R. HEELIS
DR. W. HANSON
DR. J.P. McCLURE

UTAH STATE UNIVERSITY
4TH AND 8TH STREETS
LOGAN, UTAH 84322
DR. R. HARRIS
DR. K. BAKER
DR. R. SCHUNK
DR. J. ST.-MAURICE

PHYSICAL RESEARCH LABORATORY
PLASMA PHYSICS PROGRAMME
AHMEDABAD 380 009
INDIA
P.J. PATHAK, LIBRARIAN

LABORATORY FOR PLASMA AND
FUSION ENERGY STUDIES
UNIVERSITY OF MARYLAND
COLLEGE PARK, MD 20742
JHAN VARYAN HELLMAN,
REFERENCE LIBRARIAN

END

FILMED

4-85

DTIC